

Scuola di Scienze
Dipartimento di Fisica e Astronomia
Corso di Laurea Magistrale in Fisica

The role of the cosmological constant for galactic rotation curves

Relatore:
Prof. Roberto Balbinot

Presentata da:
Matteo Magi

Correlatore:
Prof. Ruth Durrer

Anno Accademico 2019/2020

ALMA MATER STUDIORUM · UNIVERSITÀ DI BOLOGNA

Abstract

Scuola di Scienze
Dipartimento di Fisica e Astronomia

The role of the cosmological constant for galactic rotation curves

by Matteo MAGI

In questa tesi sono state studiate le curve di rotazione delle galassie a spirale all'interno dello schema concettuale dato dal modello Λ CDM, con l'intento di determinare un eventuale effetto, e la relativa portata, della costante cosmologica.

Lo studio del problema è stato condotto in accordo con la prospettiva geometrica dettata dalla teoria della relatività generale: assumendo una galassia descritta dalle soluzioni delle equazioni di campo, si sono studiate le curve di rotazione analizzando le geodetiche circolari.

Inizialmente si è esaminato un toy model di galassia, ottenuto considerando la totalità della massa concentrata in un singolo punto, studiando così la geometria dello spaziotempo di Schwarzschild-de Sitter. Si è passati poi a un modello più realistico, che tenesse conto del contributo energetico della materia oscura presente nell'alone galattico. Questa richiesta ha portato allo studio della metrica di Lemaître-Tolman. In entrambi i casi la costante cosmologica ha un effetto sulle curve di rotazione: fissata la distanza dal centro della galassia, la velocità di rotazione di una massa di prova risulta essere minore rispetto al caso in cui $\Lambda = 0$. Considerando distanze sempre maggiori si perde l'esistenza delle geodetiche circolari.

La portata di questo effetto è apprezzabile su scale dell'ordine di centinaia di kiloparsec fino a qualche megaparsec, risultando dunque di difficile osservazione necessitando di galassie isolate ben accessibili sperimentalmente. Qualora l'effetto fosse confermato, tuttavia, questo lavoro permetterebbe una nuova misura indiretta della costante cosmologica.

Acknowledgements

I have worked on this thesis during an exchange semester at the University of Geneva, I consider myself extremely lucky for the opportunity I have been given and for all I could learn in such relatively short period; it is, therefore, essential for me to express here my gratitude.

I would first like to thank my supervisor Prof. Durrer for formulating a research topic suitable to the time available, for all the consideration and invaluable guidance given throughout the project; thank you for your patience, for always finding time for me and for making me realize what it means to do research. I also need to acknowledge all the members of the Geneva Cosmology and Astroparticle physics group for the warm welcome and kindness, as well as technical help that you were always ready to give; in particular, I want to thank Adrian and Daniel for the countless conversations we had at the cafeteria.

I would also like to thank sincerely my friends and flatmates Gao, Camelia, and Tessy for the precious support you gave me and for all the time we have spent together. In addition, I would like to thank heartily my friend Thea for making me discover the wonders of your marvelous city and for truly making me feel as I belonged there.

Finally, I cannot leave out my friends in Italy, and most importantly my parents and grandparents, who despite the distance I could always feel close to me.

Contents

Abstract	iii
Acknowledgements	v
Introduction	1
1 Rotation Curves of Galaxies: Theory and Observations leading to the ΛCDM Model	5
1.1 Galaxies: a brief overview	5
1.2 Measuring Rotation Curves of Spiral Galaxies	7
1.3 The Missing Mass Problem and Dark Matter	10
1.4 Dark Energy and the Cosmological Constant	11
2 Spherically Symmetric Vacuum Solutions of Einstein Field Equations with $\Lambda > 0$	15
2.1 Spherically symmetric Lorentzian spacetime	16
2.2 Cartan's formalism for Einstein Field Equations	17
2.2.1 Vacuum Solutions	21
2.3 Generalized Birkhoff's Theorem with $\Lambda > 0$	23
2.4 Schwarzschild-de Sitter Circular Geodesics	26
2.5 Schwarzschild-de Sitter solution in Conformally Flat Coordinates	29
2.5.1 Spiral Geodesics	32
2.6 Rotation Curves seen by a far-away geodesic observer	34
3 Spherically Symmetric Inhomogeneous Solutions of Einstein Field Equations with $\Lambda > 0$	39
3.1 Spherically symmetric inhomogeneous models	39
3.2 The Lemaître-Tolman Solution	41
3.3 Curvature Coordinates for the Lemaître-Tolman Solution	44
3.3.1 Circular Geodesics	49
3.4 Numerical Analysis	53
Conclusions	58
A Nariai solution	61
Bibliography	63

List of Figures

1.1	A schematic representation of the Milky Way and its components. Image taken from the web. (http://science.marshall.edu/saken/PS101/Notes/Chapter14/OLD/milkyway1.htm)	6
1.2	NASA/ESA Hubble Space Telescope image of the spiral galaxy NGC 2903. Image taken from the web. (https://www.nasa.gov/image-feature/goddard/2019/hubble-spots-stunning-spiral-galaxy)	7
1.3	Rotation curves of sample galaxies. Model rotation curves of the individual components are also shown: the dashed curves are for the visible components, the dotted curves for the gas, and the dash-dot curves for the dark halo (see K.G. Begeman, 1991).	9
2.1	SdS metric component $g_{00} = f(r)$	22
2.2	SdS vs Schwarzschild rotation curves in linear scale.	29
2.3	SdS vs Schwarzschild rotation curves in bilogarithmic scale.	29
2.4	Spiral geodesics	33
2.5	Far-away observer O receiving light from the emitting source S given by the hydrogen atom. The whole dynamics takes place on the equatorial plane.	35
3.1	Rotation curve for FR profile.	55
3.2	Rotation curve for NFW profile.	55
3.3	Rotation curve for FR profile for vanishing and non-vanishing Λ at large radii.	56
3.4	Rotation curve for NFW profile for vanishing and non-vanishing Λ at large radii.	56
3.5	Behaviors of the mass functions with both profiles and \tilde{M} in bilogarithmic scale.	57

List of Tables

1.1	Spiral galaxies sample (see K.G. Begeman, 1991).	8
2.1	Radial displacement after 2π rotation.	33

List of Abbreviations

EFE	Einstein Field Equations
SdS	Schwarzschild-de Sitter
LT	Lemaître-Tolman
NFW	Navarro-Frenk-White
FR	Flat Rotation

Physical Constants

Parsec	$\text{pc} = 3.085\,67 \times 10^{16} \text{ m}$
Solar Mass	$M_{\odot} = 1.988\,47 \times 10^{30} \text{ kg}$
Speed of Light	$c = 2.997\,92 \times 10^8 \text{ m s}^{-1}$
Gravitational constant	$G = 6.674\,30 \times 10^{-11} \text{ m}^3 \text{ kg}^{-1} \text{ s}^{-2}$

Introduction

“Both religion and science need for their activities the belief in God, and moreover God stands for the former in the beginning, and for the latter at the end of the whole thinking. For the former, God represents the basis, for the latter – the crown of any reasoning concerning the world-view.”

Planck, 1968

Among all the branches of physics, there is one field for which this quote is of particular significance: cosmology.

In the words of Planck, we could rephrase the development of this discipline as the progressive shift of God’s position within the cosmologist’s reasoning, which eventually led to the establishment of modern cosmology.

Since time immemorial, humanity has always been overwhelmed by the unconceivable nature of Nature and immediately started to wonder about its position in the Universe. Early cosmology arose as a reassuring way to make the cosmos accessible to the human mind, and mythology was its language.

Despite the impressing observational and computational achievements of pre-scientific societies (e.g. Ptolemaeus, c. 150 AD), it was unimaginable to employ that kind of knowledge to study the Universe, in fact, the ideological frame built up by early cosmology allowed to interpret any aspect of existence in strictly human terms, leaving no space for science (for further reference see Hawley J. F., 2005).

On the other hand, modern cosmology is by all rights an observational science, which however gained this status only relatively recently, less than a century ago.

For this transition to happen, it has been necessary that cosmology deprived itself of all metaphysical facets and defined a precise domain of competence, as well as a method. To achieve this goal it has been of crucial importance the Scientific Revolution, as it is well testified by the famous and emblematic words of Newton “Hypotheses non fingo” (Newton, 1713). Ultimately, modern cosmology affirmed itself as Physical Cosmology, i.e the study of the origin, structure, evolution, and ultimate fate of the Universe, without addressing issues like the creation of the Universe itself.

The historical development of this field has been so slow compared to other scientific disciplines because of the profound conceptual meaning of the subject and, consequently, the natural reluctance to abandon a set of beliefs on which one’s existence is based upon. The endeavoring process of gradually overcome paradigms, setting new frameworks, passed through the lives of highly peculiar individuals that fearlessly faced and contested the previously established ideological system.

From Copernicus, Galileo, Kepler, Newton, we would finally have Einstein, who in 1915 set the most accurate and currently most employed mathematical framework to understand gravity: the theory of general relativity.

The real game-changer, however, happened in 1923. Before that year, in fact, it was not clear whether the Universe was much larger than the Milky Way or not. In 1923 astronomers managed to measure the distance between our galaxy and Andromeda Galaxy, pinning down individual stars, in particular those called Cepheid variables, i.e. stars that pulsate radially and exhibit a strong period-luminosity correlation. Exploiting this characteristic revealed that, indeed, Andromeda does not belong to the Milky Way, and it is about 2.5 million light-years away from us (see J. Binney, 1998), which in turn implies that the Universe must be much larger than our own galaxy.

Within eight years, the astronomer Hubble managed to observe many of these galaxies. He did not only measure their distance but also their velocities. Counterintuitively he found a law, the Hubble's law, stating that the farthest a galaxy is, the fastest it is receding from us.

The ultimate sign that a science was born can be seen from the interpretation of the Hubble's law: from the evidence, we must conclude that the Universe is expanding, abandoning all prejudices and the need of an eternal and static Universe.

Despite the late affirmation of modern cosmology, we are lucky enough to have already collected plenty of different observations, like the cosmic microwave background (CMB), the baryon acoustic oscillations (BAO), and the supernovae (SN). Now, putting these together we arrive, in the late 90s, at the formulation of the Λ CDM Model, which is the standard model to address Physical Cosmology within the scientific community, capable to describe many properties of the cosmos as we understand it today, but still far from a comprehensive picture.

The main elements of such picture are summarized as follows (for further reference see Peeble, 1993 and Durrer, 2008).

- The mass distribution of the Universe is close to homogeneous in the large-scale average, independently of the direction of observation. Fluctuations in the mass distribution averaged over volumes comparable in size to the Hubble length $\approx 4000Mpc$ are bounded by $\delta M/M \lesssim 10^{-4}$. The mass fluctuations become of order one when the smoothing radius is reduced to about one percent of the Hubble length. In other words, on sufficiently large scales, our Universe appears homogeneous and isotropic; this fact usually goes under the name of the Cosmological Principle.
- The Universe is expanding, in the sense that the mean distance l between conserved particles is increasing with time at the rate

$$\frac{dl}{dt} = H_0 l \quad (1)$$

Where the proportionality factor is the Hubble's constant evaluated today, which defines the Hubble length: $L_H = c/H_0 \approx 4000Mpc$.

- The energy content of the Universe can be split into three contributions: radiation (or any kind of massless particle), nonrelativistic matter, divided in baryonic matter and non-baryonic cold dark matter, and dark energy associated to a cosmological constant, responsible for the accelerated expansion of the Universe. If we consider these contributions as independent, meaning that

each one satisfies its own equation of state, we can quantify the entity of each contribution through a dimensionless density parameter Ω .

The fraction of the total energy density made of dark energy is estimated to be $\Omega_\Lambda = 0.669 \pm 0.038$, based on the 2018 Dark Energy Survey results using Type Ia Supernovae (see Maeder, 2018a) or $\Omega_\Lambda = 0.6847 \pm 0.0073$, based on the 2018 release of Planck satellite data (see Maeder, 2018b). Instead, baryonic matter, which is all we can describe with the standard model of Particle Physics, accounts only for roughly the 5% of the mass-energy density of the Universe (see L. Amendola, 2010).

- Our Universe is mathematically described by a four-dimensional spacetime (\mathcal{M}, g) given by a Lorentzian manifold \mathcal{M} with metric g , that is a solution of Einstein field equations. To take into account the Cosmological Principle such spacetime needs to be homogeneous and isotropic, i.e. it must admit slicing in maximally symmetric 3-spaces; this type of solution is known as Friedman-Lemaître universe.

Another consequence of the Cosmological Principle and the observation that the Universe is expanding, is that if we extrapolate backwards such expansion, we encounter a singularity in the solutions of Einstein field equations, assuming ordinary physics to hold. This implies an origin of time, which we call Big Bang.

It is precisely in this conceptual scheme that we want to revisit one of the crucial problems at the base of the Λ CDM Model itself: in the late 1960s a team of astronomers, with a major role played by Vera Rubin, studied the rotation curves of spiral galaxies and contributed to the discovery of the dark matter.

Typically, the information given by galactic rotation curves is understood in Newtonian terms; instead, what we have studied in this thesis is a contextualization of the problem within the Λ CDM Model, with particular emphasis on the role played by the cosmological constant.

The work will be structured as follows: in the first chapter we will first present the main features of galaxies, with special focus on spiral galaxies and their components' dynamics, we will then be able to address the problem of rotation curves and we will present the generally accepted solution of the missing mass problem in a Newtonian framework. We will finally complete the standard picture of the Λ CDM Model discussing dark energy and the cosmological constant. In this preliminary chapter, we will strongly refer to J. Binney, 1998 unless otherwise explicitly stated.

In the second chapter, we will begin our analysis translating the observational problem in the geometrical framework given by general relativity. We will start with a well-defined and simplified model for a spiral galaxy, studying spherically symmetric vacuum solutions of Einstein field equations (EFE) with positive cosmological constant, and we will give analytical results regarding theoretical rotation curves.

In the third chapter, we will investigate a more realistic model of a spiral galaxy, studying spherically symmetric inhomogeneous solutions of EFE with positive cosmological constant. We will therefore present Lemaître-Tolman solution, and we will study rotation curves analyzing the circular geodesics in curvature coordinates.

In the following, the mostly-minus metric signature will be employed, and we will always work in such units that the speed of light and the gravitational constant are

set to one. In these units, times and masses are measured in kiloparsecs via the conversion relation $2M_{\odot}G/c^2 = 10^{-16}kpc$.

The EFE take the form:

$$G_{\mu\nu} := R_{\mu\nu} - \frac{1}{2}Rg_{\mu\nu} = 8\pi T_{\mu\nu} + \Lambda g_{\mu\nu} \quad (2)$$

Where $G_{\mu\nu}$ is the Einstein tensor and it is defined in terms of the Ricci tensor $R_{\mu\nu}$ and the Ricci scalar R , $T_{\mu\nu}$ is the energy-momentum tensor, Λ is the cosmological constant and $g_{\mu\nu}$ the spacetime metric. We will assume for the cosmological constant the value $\Lambda = 10^{-13}kpc^{-2}$ (see L. Amendola, [2010](#)).

Chapter 1

Rotation Curves of Galaxies: Theory and Observations leading to the Λ CDM Model

1.1 Galaxies: a brief overview

We can think of a galaxy as a gravitationally bound collection of stars, gas, and dust. Such systems, which in turn are arranged into bound clusters and still larger structures, can contain from 10^7 to 10^{12} stars, reaching a total luminous mass of roughly $10^{11} M_{\odot}$, and a diameter of up to the order of $0.1 Mpc$. The gas component typically accounts for the ten percent of the stellar mass, while the dust component for the one percent of the gaseous mass.

Historically, galaxies have often been at the center of scientific debates, in fact, as they provide one of the most visually stunning phenomena in the night sky, early astronomers always wondered about their nature. Since the first decades of the 20th century, however, we know that there exist countless of these systems in the Universe, and our Milky Way has no extraordinary properties.

Galaxies can exhibit a rich variety of characteristics such as size, luminosity and dynamics, therefore many classification schemes, based on different criteria, have been proposed during the years. The most employed one was introduced by Hubble in 1936: for our purposes, we will focus just on what he defined "spiral galaxies", without going into too many details.

Spiral galaxies, as their name suggests, are named after their morphology: let us now briefly describe their main components.

- *Bulge*. Central brightness condensation with a diameter of the order of few kiloparsecs, at the center of which a supermassive black hole presumably resides, it is mostly made of old stars (Population II). From this site more or less conspicuous spirals of enhanced luminosity, the spiral arms, extend outwards into the galactic disc.
- *Galactic disk*. Rotating disk of hundreds of parsecs width and tens of kiloparsecs of extension, it contains stars (Population I and II), dust and the majority of the atomic and molecular cold gas, associated with star formation. The main features of the disk are the spiral arms that are sites of ongoing star formation and are brighter than the surrounding disc because of the young, hot OB stars that inhabit them.

- *Halo*. A nearly spherical halo that surrounds the galaxy, it is mainly made of hot gas and few Population II stars belonging to globular clusters. This halo is in turn surrounded by a larger, still nearly spherical, very massive halo of dark matter with a radius of hundreds of kiloparsecs.

This component is of central importance for this thesis therefore it will be discussed in more detail later on: in this chapter, we will deal mainly with its discovery.

The surface brightness profiles of the galactic disk follow very closely exponential functions in both the radial and vertical directions showing how the majority of the stars belong to the inner part of the disk while the gaseous component is observed also in the outer parts.

Many of the spiral galaxies observed have an additional bar-like structure extending from the central bulge: our own Milky Way is, in fact, a barred spiral with a disk diameter of roughly $30kpc$.

FIGURE 1.1: A schematic representation of the Milky Way and its components.
Image taken from the web.
(<http://science.marshall.edu/saken/PS101/Notes/Chapter14/OLD/milkyway1.htm>)

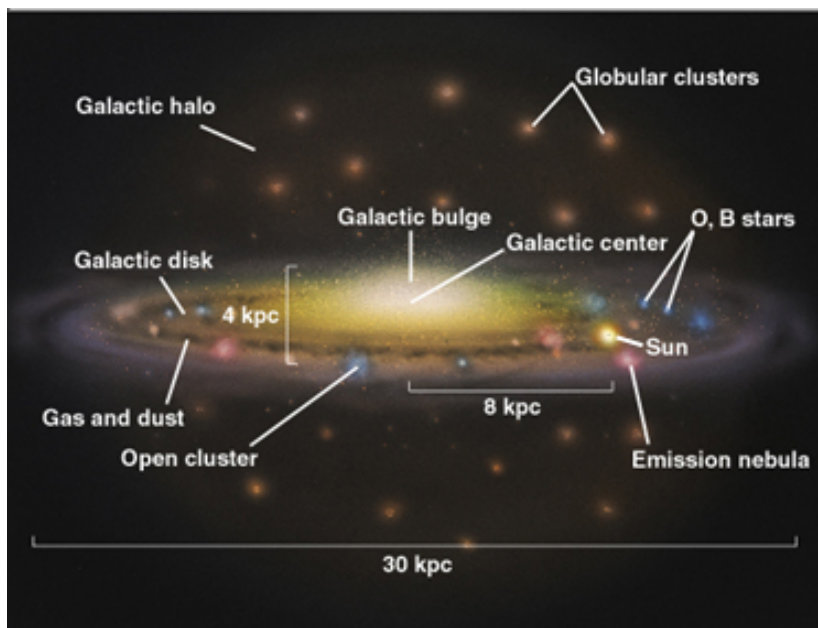
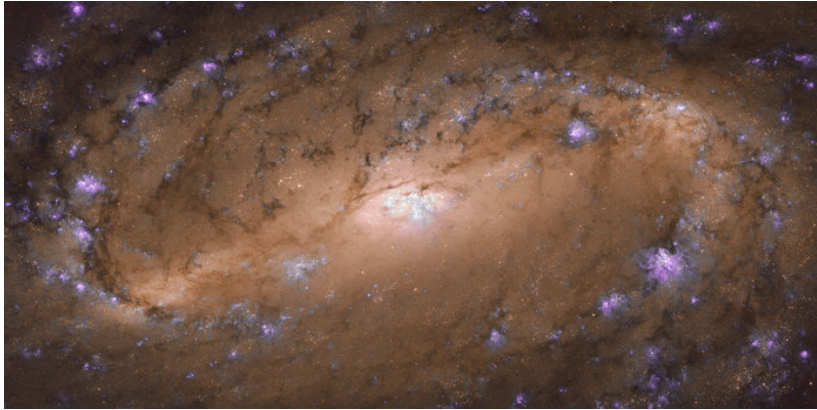


FIGURE 1.2: NASA/ESA Hubble Space Telescope image of the spiral galaxy NGC 2903. Image taken from the web.
(<https://www.nasa.gov/image-feature/goddard/2019/hubble-spots-stunning-spiral-galaxy>)



1.2 Measuring Rotation Curves of Spiral Galaxies

When measuring the kinematics of individual stars, astronomers use the Doppler shift of each star's spectral emission lines to measure its line-of-sight velocity. If the star is moving with line of sight velocity v_{los} , then the spectrum of the star will reveal that a feature which naturally occurs at wavelength λ , will be shifted by $\Delta\lambda = (v_{los}/c)\lambda$ (since $v_{los} \ll c$). This procedure applies to all kinds of spectral lines, and what these observations have shown, is that stars undergo rotational motions around the galactic center and the rotation is differential, meaning that the angular velocity is a function of the position as well.

However, the most accurate information on the behavior of rotation curves at large radii is obtained from external galaxies and, in this case, individual stars cannot usually be optically resolved, and the majority of the starlight from an external galaxy forms an unresolved continuum. These technical issues are not relevant for this thesis, what instead is worth mentioning is the result that kinematic studies of external spiral galaxies reveal that, in all but face-on systems, the stars follow approximately circular orbits with little random motion.

Early measurements of rotation curves date back to the 1950s and 1960s with the study of emission lines in H II regions, these are regions where the hydrogen is ionized due to the UV radiation of young stars, and the consequent emission is well visible at the optical wavelength of $656.3nm$. The results typically showed a steep rise in the rotation speed near the galactic center, and then a short level section before the last data point was reached.

From the 1970s the situation changed: thanks to the improvements made in radio astronomy, it was possible to extend the rotation curves to radii larger than the optical disk using the 21-cm emission line of the neutral hydrogen in HI regions.

The ground state of the atomic hydrogen is split into two hyperfine levels by the interaction between the spins of the electron and the proton in such a way that the actual ground state has total angular momentum zero, and there are three degenerate states with total angular momentum one. The transition between the two levels, mediated by photons with a wavelength of $21.105cm$, is in fact "forbidden" due to

the electric dipole moment selection rules, but it is significantly present thanks to environmental conditions.

These measurements displayed that the rotation curves for the gaseous component have similar properties to those obtained from the stars, and they can be traced even in the outer part of the disk where the stellar component is very faint. At these radii, almost all spiral galaxies have flat rotation curves or slowly rising out to the last measured point of few tens of kiloparsecs, very few show falling rotation curves.

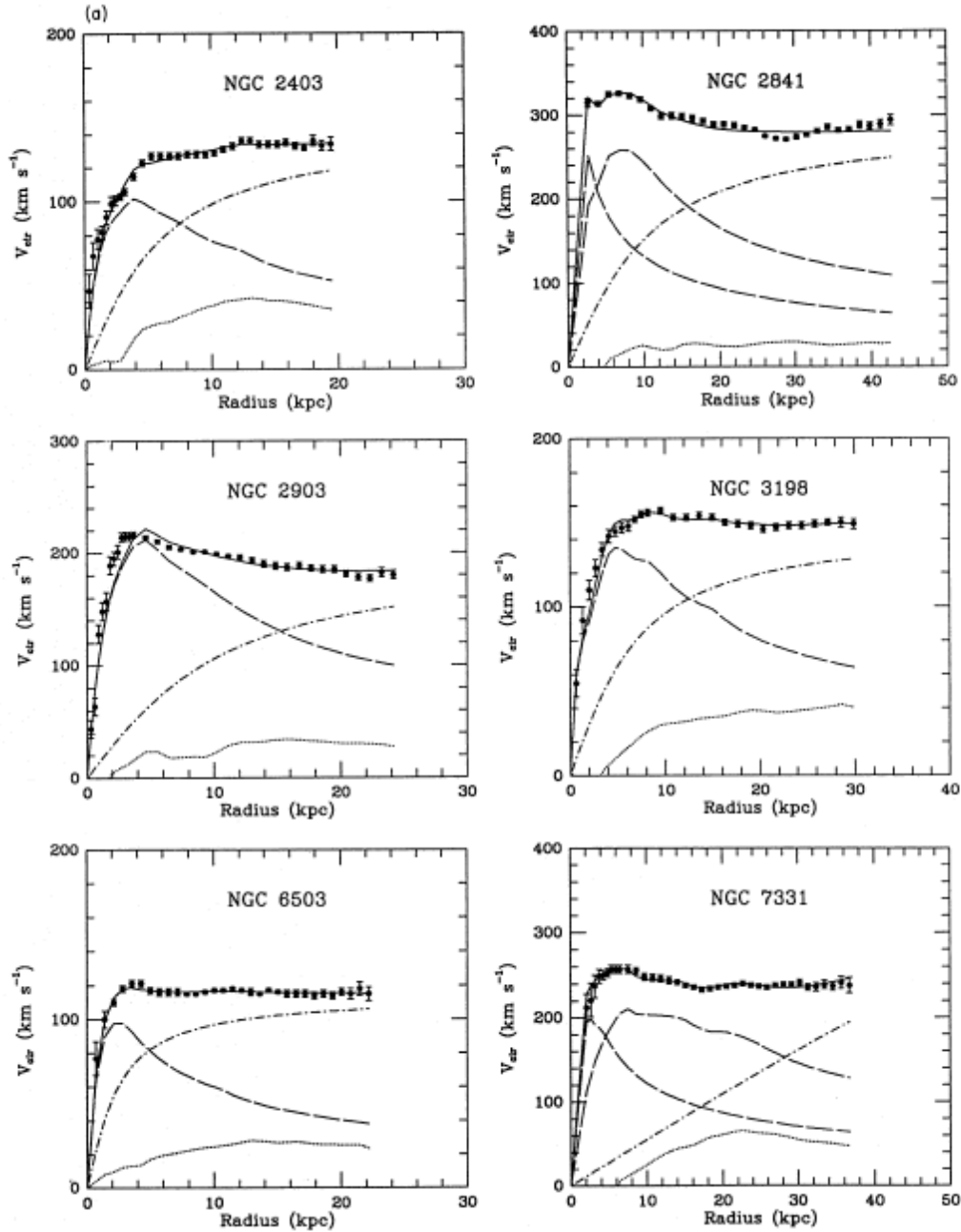
We will present here some of these data relative to spiral galaxies taken from (K.G. Begeman, 1991).

TABLE 1.1: Spiral galaxies sample (see K.G. Begeman, 1991).

Galaxy	Luminosity Mass ($10^9 M_{\odot}$)	Distance to M81 group (Mpc)	R_{25} (kpc)	R_{HI} (kpc)
NGC 2403	7.90	3.25	8.41	19.49
NGC 2841	20.50	9.46	11.28	42.63
NGC 2903	15.30	6.40	11.73	24.18
NGC 3198	9.00	9.36	11.44	29.92
NGC 6503	4.80	5.94	5.36	22.22
NGC 7331	54.00	14.90	23.40	36.72

R_{25} is a photometric quantity which gives in good approximation the optical radius of the galaxy and R_{HI} is the last measured point of the rotation curve obtained from the 21-cm line of neutral hydrogen.

FIGURE 1.3: Rotation curves of sample galaxies. Model rotation curves of the individual components are also shown: the dashed curves are for the visible components, the dotted curves for the gas, and the dash-dot curves for the dark halo (see K.G. Begeman, 1991).



The reason why these plots are so remarkable will be addressed in the next section. Let us now make a crucial point: as shown in these pictures the typical speed of stars and gas in a circular orbit is about 200 km s^{-1} , in astronomical units this means almost two hundreds parsecs per megayear, thus the time required to complete one orbit of 10 kpc of radius is roughly 300 Myr . Since the age of a galaxy is about ten gigayears, most stars in spiral galaxies have completed over thirty revolutions and it is therefore reasonable to assume that the galaxies are now in an approximately steady state. Finally, we want to stress the fact that the orbital period is a factor 10^5 or

10^6 times larger than the interval over which observations have been recorded. This means that we are forced to base our understanding of galactic structures on what appears to be an instantaneous snapshot of the system (for reference of the whole paragraph see J. Binney, 1987).

1.3 The Missing Mass Problem and Dark Matter

All this interest on rotation curves is motivated by the fact that they provide the most direct method of measuring the mass distribution of a galaxy.

If we consider a gravitationally bound system, such as the Solar System, and we assume the validity of Kepler's laws, we know that a mass orbiting around the Sun satisfies the equation of motion:

$$\frac{GM_{\odot}}{R^2} = \frac{v^2}{R} \implies v(R) = \sqrt{\frac{GM_{\odot}}{R}}, \quad (1.1)$$

where G is the gravitational constant, M_{\odot} is the mass of the Sun, v is the tangential velocity and R the distance of the mass from the Sun.

This argument could be generalized to a smooth azimuthally symmetric density distribution with a finite mass that models the spiral galaxy as a rigid body. This would predict rotation curves in which are present: an inner region in which the speed rises with the distance from the center, a region in which the speed reaches a maximum and begins to decline, and a Keplerian region in which the rotation speed falls accordingly with the previous equation as $R^{-1/2}$.

This situation is far from reality; therefore an interpretation of the flat rotation curve is needed, as there is something fundamental that cannot be understood with previous knowledge. In particular, it appears from the measure of rotation curves that no spiral galaxy has a well-determined total mass.

Before proceeding let us take a step back. Before the accurate measurements of the rotation curves, the determination of the mass of galaxies was already a puzzle.

One of the quantities that astronomers like to deal with is the mass-to-light ratio: taking the Sun as reference, we define its mass-to-light ratio, i.e. mass over luminosity, to be one $Y_{\odot} = 1$. If we now consider a thousand stars like the Sun, the total mass-to-light ratio would still be one as the masses and the luminosities are simply added. Regarding galaxies astronomers still expected to find a mass-to-light ratio of order one even in regions of smaller luminosity density, such as the outer parts of the galaxy. This conjecture, however, proved to be very wrong as these outer parts have much larger mass-to-light ratios, in some cases also one order of magnitude higher than the inner parts.

This discrepancy went down in history as the "missing mass" problem, since there was no candidate source able to explain the measured value.

The first serious attempt to solve the problem was proposed by the Swiss astronomer Fritz Zwicky, who compared the mass information given by the dispersion velocities of galaxies in the Coma cluster with the observable star mass, and proposed the hypothesis that the discrepancy was due to some undetectable matter, "Dunkle Materie", which only interacted gravitationally. This theory did not have immediate credit also because of Zwicky's inaccurate methodology (see J. Binney, 1987).

However, it was in the late 1970s, when Vera Rubin obtained detailed measures of the rotation curves (see V.C. Rubin, 1980) of Andromeda Galaxy, that Zwicky's theory got back in the scene. It proved in fact to be the simplest interpretation opposed to a modification of Newtonian theory, and was therefore generally accepted by the scientific community, keeping Zwicky's denomination "dark matter".

Nowadays it is widely believed that spiral galaxies possess halos of dark matter, so-called dark halos, that extend to much larger radii than the optical disk.

If we approximate the dark halo as spherical, and we consider sufficiently large radii that the gravitational force from the disk can be neglected, then a rotation curve of constant tangential velocity implies that the halo mass increases linearly with the distance from the center:

$$\frac{dM}{dR} = 4\pi R^2 \rho(R) = \frac{v^2}{G} \quad (1.2)$$

where now v is a constant. Let us rephrase this result in terms of the angular momentum for unit mass of a particle that moves in the gravitational potential of the dark halo. Since gravity, which is a central force, is the only force it is subject to, the angular momentum is a conserved quantity: $J = Rv$. This means that the angular momentum has the same functional behavior as the dark halo mass.

1.4 Dark Energy and the Cosmological Constant

We will conclude this chapter giving some more details on the Λ CDM Model assuming the reader is already familiar with some astronomical and cosmological concepts (for further reference see L. Amendola, 2010).

One of the early key observations that initiated modern cosmology is attributed to Edwin Hubble, who, in 1929, measuring the recession velocities of distant galaxies, provided one of the first evidences of the expansion of the Universe, described by the already presented Hubble law. Subsequently, many other observations took place, having the aim not only to confirm the expansion of the Universe but also to measure the rate of this expansion. Since 1998, these measurements became very accurate and gave convincing evidence of a late-time cosmological acceleration. The source of this acceleration is associated to what we call "dark energy".

Nowadays the existence of dark energy is supported by several observations such as the age of the Universe compared to oldest stars, supernovas type Ia (SN Ia), cosmic microwave background (CMB), baryon acoustic oscillations (BAO), and large-scale structure (LSS).

As we have anticipated in the introduction, in modern cosmology we describe our Universe via the Friedmann-Lemaître solution of EFE. Without getting into the details (see Durrer, 2008), the metric g of this solution is of the form:

$$ds^2 = g_{\mu\nu} dx^\mu dx^\nu = dt^2 - a^2(t) \left[\frac{dr^2}{1 - kr^2} + r^2(d\theta^2 + \sin^2\theta d\varphi^2) \right]. \quad (1.3)$$

Where the cosmic time t is the proper time of an observer who sees a spatially homogeneous and isotropic universe, such that the 3-spaces of constant t are maximally symmetric spaces of constant curvature k ; $a(t)$ is the scale factor. Given the symmetry

of this spacetime, the energy-momentum tensor can only have the components

$$T_{\mu\nu} = -Pg_{\mu\nu} + (P + \rho)\delta_{\mu\nu}, \quad (1.4)$$

where ρ and P are respectively the energy density and the pressure of the Universe. The EFE $G_{\mu\nu} = 8\pi T_{\mu\nu}$ can be expressed in terms of ordinary differential equations for the scale factor, which are the Friedmann equations:

$$\begin{cases} \ddot{a} = -\frac{4\pi}{3}(\rho + 3P)a \\ \dot{a}^2 + k = \frac{8\pi}{3}\rho a^2 \end{cases}. \quad (1.5)$$

One of the first attempts at studying these equations was given by Einstein in 1917, who wanted to reproduce a static Friedmann-Lemaître universe, i.e. a solution with $\dot{a}(t) = 0$. From the first equation of (1.5) we see that $\rho + 3P = 0$ must be satisfied. To make sense of this relation, Einstein introduced the simplest modification to the field equations, in terms of the cosmological constant Λ , arriving at: $G_{\mu\nu} = 8\pi T_{\mu\nu} + \Lambda g_{\mu\nu}$. This leads to effective values of the energy density and the pressure:

$$\begin{cases} \rho_{eff} = \rho + \frac{\Lambda}{8\pi} \\ P_{eff} = P - \frac{\Lambda}{8\pi} \end{cases}. \quad (1.6)$$

We note that for $\Lambda > 0$, the pressure gains a negative term.

After Hubble's discovery, Einstein abandoned the idea of realizing a static universe, and regretted the cosmological constant as his "biggest blunder". Indeed, there was nothing to regret: after 1998 the cosmological constant revived again as a form of dark energy responsible for the late-time acceleration of the Universe. In fact, if we look again at the first equation in (1.5), we see that we can describe an accelerated expansion of the universe only if we assume the effective quantities ρ_{eff} and P_{eff} . In general, dark energy is described assuming a background that satisfies the equation of state $w_{DE} := P_{DE}/\rho_{DE}$ where P_{DE} is the pressure and ρ_{DE} the energy density of the dark energy. From what we have said we expect $w_{DE} < 0$ to explain the accelerated expansion of the Universe. The previously mentioned observations can test this dark energy model if we assume a constant equation of motion.

The SN Ia observations have provided information on the cosmic expansion history around the redshift $z \lesssim 2$ by the measurement of luminosity distances of the sources. The presence of dark energy leads to a shift of the position of acoustic peaks in CMB anisotropies, as well as a modification of the large-scale CMB spectrum through the so-called integrated Sachs–Wolfe effect. The combined analysis of SN Ia and CMB can provide tight bounds on the equation of state w_{DE} and the present energy fraction of dark energy $\Omega_{DE,0}$. The distribution of large-scale clustering of galaxies in the sky also provides additional information on the properties of dark energy. In 2005 the detection of a peak of baryon acoustic oscillations was reported by Eisenstein et al. at the average redshift $z = 0.35$ from the observations of luminous red galaxies in the Sloan Digital Sky Survey. This has also given another independent test of dark energy. From the combined analysis of SN Ia, CMB, and BAO, the Wilkinson Microwave

Anisotropy Probe (WMAP) group obtained the bound $-1.097 < w_{DE} < -0.858$ at the 95% confidence level. The most recent and tightest constraint is given by (see Planck, 2018): $w_{DE} = -1.028 \pm 0.031$ at the 68% confidence level.

Hence, the simplest candidate for dark energy is the cosmological constant, whose equation of state is simply given by (1.6): $w_{DE} \equiv w_{\Lambda} = -1$.

This cosmological constant solution, however, is not free from controversies. From the viewpoint of particle physics, the cosmological constant appears as a vacuum energy density. If we sum up zero-point energies of all normal modes of some field and take the cut-off scale of the momentum at the Planck scale, the vacuum energy density is estimated to be $\rho_{vac} \simeq 10^{74} GeV^4$. This is much larger than the observed value of the dark energy: $\rho_{vac} \simeq 10^{-47} GeV^4$. If vacuum energy with an energy density of the order of $\rho_{vac} \simeq 10^{74} GeV^4$ was present in the past, the Universe would have entered an eternal stage of cosmic acceleration already in the very early Universe. This is, of course, problematic because the success of the Big Bang Cosmology, based on the presence of radiation and matter epochs, would be destroyed.

Consequently, there exist alternative approaches to dark energy; here we will just mention them, as they are still ongoing research topics.

One approach is to modify the EFE by considering a specific form of the energy-momentum tensor with negative pressure, a representative model is the so-called quintessence; the other approach would be to modify the geometric related part, resulting in a class of theories of so-called modified gravity.

Chapter 2

Spherically Symmetric Vacuum Solutions of Einstein Field Equations with $\Lambda > 0$

The first task to study rotation curves of galaxies in the Λ CDM Model is to translate the observational scenario presented in the previous chapter into a mathematical framework. According to the theory of general relativity, gravity manifests itself as the geometric property of spacetime; therefore, we need to relate a spiral galaxy to a proper spacetime, i.e. to some solution of EFE.

Since we are dealing with the kiloparsec scale, we cannot rely on the Cosmological Principle to guide us. However, luckily, other known exact EFE solutions are suitable for our purposes.

This chapter aims at gaining some intuition on the problem: we will start considering a toy model of a point-like galaxy, which translates mathematically to the so-called Schwarzschild-de Sitter spacetime. We will then prove the generalized Birkhoff's theorem with positive cosmological constant to convince ourselves of the generality of this solution.

Finally, since our interest is the investigation of the rotation curves, it is immediate in this formulation to model them as circular geodesics of test particles, which are going to be the focus of this work.

2.1 Spherically symmetric Lorentzian spacetime

To work with exact solutions of EFE, it is necessary to make an additional hypothesis on the galaxies we want to study: we must restrict our attention to spherical symmetric systems, so that the gravitational field outside the galaxy is then well described by a spherical symmetric spacetime. Since this assumption is at the base of the whole work, let us devote a section to give a proper introduction. In doing so, we will also take the chance to introduce some of the mathematics employed throughout the document, assuming however basic knowledge of differential geometry.

From the Einstein Equivalence Principle, we know that the mathematical model for spacetime (i.e. the set of all elementary events) in the presence of gravitational fields is a pseudo-Riemannian manifold \mathcal{M} , whose metric g has the same signature as the Minkowski metric $\eta := \text{diag}(1, -1, -1, -1)$. The pair (\mathcal{M}, g) is called a Lorentzian manifold and g is called a Lorentzian metric.

Given this manifold let us define $\mathcal{I}_s^r(\mathcal{M})$ the set of tensor fields of rank (r, s) on \mathcal{M} , and $\mathcal{I}(\mathcal{M}) = \sum_{r,s=0}^{\infty} \mathcal{I}_s^r(\mathcal{M})$ is the tensor algebra over the field of real numbers \mathbb{R} .

If ϕ is a diffeomorphism of \mathcal{M} to itself, we know that the push-forward ϕ_* is a linear isomorphism between the tangent spaces $\mathcal{T}_{\phi^{-1}(x)}(\mathcal{M})$ and $\mathcal{T}_x(\mathcal{M})$, where x is a point of \mathcal{M} .

In general it can be shown that there exists a one-to-one correspondence between linear isomorphisms on vector spaces V and W , and algebraic isomorphisms on tensor algebras $T(V)$ and $T(W)$ that preserve the rank and commute with contractions. In our case we can say that ϕ induces an automorphism on the algebra $\mathcal{I}(\mathcal{M})$, and we will call it $\tilde{\phi}$.

If T is a tensor field on \mathcal{M} , we can define the Lie derivative of T with respect to a vector field X the application from $\mathcal{I}(\mathcal{M})$ to itself, that maps T in $L_X T$ as follows:

$$(L_X T)_x = \lim_{t \rightarrow 0} \frac{1}{t} [T_x - (\tilde{\phi}_t T)_x] \equiv \lim_{t \rightarrow 0} \frac{1}{t} [T_x - \tilde{\phi}_t(T_{\phi_t^{-1}(x)})], \quad (2.1)$$

where ϕ_t is the (local) transformation that induces X .

With this definition the Lie derivative is a derivation of $\mathcal{I}(\mathcal{M})$ that preserves the rank and commutes with contractions. In addition, it acts on any smooth function f and any vector field Y as:

$$\begin{cases} L_X f = Xf \\ L_X Y = [X, Y]. \end{cases} \quad (2.2)$$

Among the key properties of the Lie derivative we also have to recall that $L_{[X,Y]} = [L_X, L_Y]$ holds.

In general we say that a tensor field T is invariant under the action of a vector field X if $L_X T = 0$; it is easy to see that from the linearity of the Lie derivative, and thanks to the equation above, the set of vector fields under which T is invariant form a Lie algebra.

If T is the metric tensor g , then these vector fields are called Killing vector fields, and are denoted with the letter K . A Lie group whose Lie algebra is the Lie algebra of Killing vector fields is called isometry group of the manifold \mathcal{M} .

Finally, we define a manifold \mathcal{M} to be spherically symmetric if the Lie algebra of Killing vector fields contains a subalgebra which is the Lie algebra of the group $\text{SO}(3)$,

i.e. if it admits the group $SO(3)$ as an isometry group. If these Killing fields are defined only in open neighborhoods of every point x , and cannot be extended to the whole manifold, we say that the spacetime is locally spherically symmetric.

Given a Lie group we can define the orbit of $x \in \mathcal{M}$ as the set of points in \mathcal{M} that can be reached by x through the action of the group transformations. Hence, for a Lorentz spherical symmetric manifold we can say that the $SO(3)$ isometry group orbits are two-dimensional spacelike surfaces. It can be shown (for details see Straumann, 2005) that the manifold \mathcal{M} can be expressed, at least locally, as a warped product:

$$\mathcal{M} = \widetilde{\mathcal{M}} \times_R S^2, \quad (2.3)$$

where $\widetilde{\mathcal{M}}$ is a 2-dimensional Lorentz manifold and ${}_R S^2$ the 2-sphere of radius R . This means that the metric takes the form:

$$g = \widetilde{g} + R^2 \widehat{g}, \quad (2.4)$$

where \widetilde{g} is the metric on $\widetilde{\mathcal{M}}$ and \widehat{g} the S^2 standard metric.

With these remarks we can introduce local coordinates $(\tilde{t}, \tilde{r}, \vartheta, \varphi)$ such that the metrics take the general form:

$$\begin{cases} g = \widetilde{g}(t, r) - R^2(t, r)(d\vartheta \otimes d\vartheta + \sin^2 \vartheta d\varphi \otimes d\varphi) \\ \widetilde{g} = \alpha d\tilde{t} \otimes d\tilde{t} + 2\beta d\tilde{t} \otimes d\tilde{r} + \gamma d\tilde{r} \otimes d\tilde{r} \end{cases}. \quad (2.5)$$

Where the functions α , β and γ satisfy the condition $\alpha\gamma - \beta^2 < 0$, since the metric is Lorentzian.

Given the tensor structure of EFE, we know that any solution g is independent from the choice of the local coordinates; therefore we are free to introduce a reparametrization in which the metric is diagonal. Let us consider the new variables (t, r) , such that:

$$\begin{cases} \tilde{t} = \zeta(t, r) \\ \tilde{r} = r \end{cases}. \quad (2.6)$$

Differentiating we find that it is possible to obtain a diagonal form for the metrics if the function ζ satisfies $\alpha \partial_r \zeta + \beta = 0$. Hence we get that it is possible to specify \widetilde{g} with only two independent functions. With proper coordinate redefinition, we arrive at:

$$g = e^{2a(t,r)} dt \otimes dt - e^{2b(t,r)} dr \otimes dr - R^2(t, r)(d\vartheta \otimes d\vartheta + \sin^2 \vartheta d\varphi \otimes d\varphi). \quad (2.7)$$

This particular choice will be useful in the following.

2.2 Cartan's formalism for Einstein Field Equations

Let us now give a further mathematical characterization of the gravitational field of a galaxy. We say that the field is stationary, if it is possible to introduce coordinates such that the metric's components do not depend on the time coordinate. However, this can be translated more generally into an intrinsic feature of the spacetime: the metric g of a manifold \mathcal{M} is called stationary if it admits a timelike Killing vector

field K . Moreover, a stationary spacetime is said to be static, if the 1-form associated to the Killing vector $\kappa := g(K, \cdot)$ satisfies the condition $\kappa \wedge d\kappa = 0$.

If we take $K = \partial_t$ to be the only timelike killing vector, it is possible to show that the line element of a spherically symmetric and static spacetime can be written as (for details see Straumann, 2005):

$$\begin{cases} ds^2 = f(r)dt^2 - \frac{dr^2}{f(r)} - r^2d\Omega^2 \\ d\Omega^2 = d\vartheta^2 + \sin^2\vartheta d\varphi^2 \end{cases} . \quad (2.8)$$

To express the EFE in a more convenient way than the coordinate formulation of general relativity we will work in the tetrad formulation, employing Cartan's formalism (see Straumann, 2005).

In a tetrad base, the metric's components do not depend on the spacetime coordinates, as the functional dependence is absorbed by the basis forms: we will make all the computations with respect to an orthonormal basis, such that $g_{ij} = \eta_{ij}$.

If we choose an orthonormal basis of vector fields $\{e_i\}_{i=1}^4$ in an open set $\mathcal{U} \subset \mathcal{M}$, the dual basis $\{\beta^i\}_{i=1}^4$, given by $\langle \beta^j, e_i \rangle = \delta_i^j$, can be taken as:

$$\begin{cases} \beta^0 = \sqrt{f(r)}dt \\ \beta^1 = \frac{dr}{\sqrt{f(r)}} \\ \beta^2 = rd\vartheta \\ \beta^3 = r \sin\vartheta d\varphi \end{cases} . \quad (2.9)$$

After exterior differentiation, we get:

$$\begin{cases} d\beta^0 = \frac{1}{2} \frac{f'(r)}{\sqrt{f(r)}} \beta^1 \wedge \beta^0 \\ d\beta^1 = 0 \\ d\beta^2 = \frac{\sqrt{f(r)}}{r} \beta^1 \wedge \beta^2 \\ d\beta^3 = \frac{1}{r} \left(\sqrt{f(r)} \beta^1 \wedge \beta^3 + \cot\vartheta \beta^2 \wedge \beta^3 \right) \end{cases} . \quad (2.10)$$

Let us now consider an affine connection on the manifold \mathcal{M} . We recall that an affine connection can be thought of as a rule for parallel transport on \mathcal{M} : given a curve G , a vector field U tangent to G and another vector field V , we say that the vector V has been parallel transported along G if

$$\nabla_U V = 0, \quad (2.11)$$

Where ∇_U is the covariant derivative along the vector field U . The covariant derivative can be defined in a similar fashion to the Lie derivative; therefore, we will omit the details (see Straumann, 2005). The main difference with the Lie derivative is that

now we do not need to know the vector fields U and V on a neighborhood of G , but just on the curve itself, as well as the affine connection on it.

Given a vector basis we can completely characterize the affine connection if we specify the Christoffel symbols Γ_{ji}^k :

$$\nabla_{e_i} e_j = \Gamma_{ji}^k e_k \equiv \langle \omega^k_j, e_i \rangle e_k. \quad (2.12)$$

Where we have introduced the connection 1-form $\omega^k_j = \Gamma_{jm}^k \beta^m$.

It is also possible to fully describe the affine connection in terms of tensor quantities. To do so let us introduce two quantities: the torsion, which is a (1,2) tensor given by:

$$T(e_i, e_j) = \nabla_{e_i} e_j - \nabla_{e_j} e_i - [e_i, e_j] \equiv \Theta^k(e_i, e_j) e_k \quad (2.13)$$

and the Riemann curvature, a (1,3) tensor:

$$R(e_i, e_j) e_k = ([\nabla_{e_i}, \nabla_{e_j}] - \nabla_{[e_i, e_j]}) e_k \equiv \Omega^m_k(e_i, e_j) e_m. \quad (2.14)$$

Where we have introduced the torsion and curvature 2-forms: $\Theta^k(e_i, e_j) = T_{ji}^k$, $\Omega^m_k(e_i, e_j) = R_{kij}^m$.

These forms are related by the following theorem:

Theorem 1. *The torsion and curvature 2-forms satisfy Cartan's structure equations:*

$$\begin{aligned} \Theta^i_j &= d\beta^i + \omega^i_j \wedge \beta^j \\ \Omega^i_j &= d\omega^i_j + \omega^i_k \wedge \omega^k_j \end{aligned} \quad (2.15)$$

Since we are considering a Lorentz manifold, it is customary to assume a Levi-Civita connection. This is the only possible symmetric (i.e. with vanishing torsion) affine connection compatible with the metric (i.e. with vanishing covariant derivative of the metric tensor).

This means that the first set of structure equations become $d\beta^i + \omega^i_j \wedge \beta^j = 0$, and we also have $dg_{ij} = g_{im}\omega^m_j + g_{jm}\omega^m_i := \omega_{ij} + \omega_{ji}$.

If we consider now (2.9) and (2.10), we can find the connection 1-forms in our tetrad basis:

$$\left\{ \begin{array}{l} \omega^0_1 = \omega^1_0 = \frac{1}{2} \frac{f'(r)}{\sqrt{f(r)}} \beta^0 \\ \omega^0_2 = \omega^2_0 = \omega^0_3 = \omega^3_0 = 0 \\ \omega^2_1 = -\omega^1_2 = \frac{\sqrt{f(r)}}{r} \beta^2 \\ \omega^3_1 = -\omega^1_3 = \frac{\sqrt{f(r)}}{r} \beta^3 \\ \omega^3_2 = -\omega^2_3 = \frac{\cot \vartheta}{r} \beta^3 \end{array} \right. \quad (2.16)$$

Via the second set of structure equations, we then obtain the curvature 2-forms:

$$\begin{cases} \Omega^0_1 = \mathcal{E}\beta^0 \wedge \beta^1 \\ \Omega^0_2 = \tilde{\mathcal{E}}\beta^0 \wedge \beta^2 + \mathcal{H}\beta^1 \wedge \beta^2 \\ \Omega^0_3 = \tilde{\mathcal{E}}\beta^0 \wedge \beta^3 + \mathcal{H}\beta^1 \wedge \beta^3 \\ \Omega^1_2 = \tilde{\mathcal{F}}\beta^1 \wedge \beta^2 - \mathcal{H}\beta^0 \wedge \beta^2 \\ \Omega^1_3 = \tilde{\mathcal{F}}\beta^1 \wedge \beta^3 - \mathcal{H}\beta^0 \wedge \beta^3 \\ \Omega^2_3 = \mathcal{F}\beta^2 \wedge \beta^3 \end{cases} \quad (2.17)$$

We have introduced the functions $\mathcal{E}, \tilde{\mathcal{E}}, \mathcal{F}, \tilde{\mathcal{F}}, \mathcal{H}$ that will be useful in a following section. In this case:

$$\begin{cases} \mathcal{E} = -\frac{f''(r)}{2} \\ \tilde{\mathcal{E}} = -\frac{f'(r)}{2r} \\ \mathcal{H} = 0 \\ \mathcal{F} = \frac{1-f(r)}{r^2} \\ \tilde{\mathcal{F}} = -\frac{f'(r)}{2r} \end{cases} \quad (2.18)$$

The Ricci tensor is obtained using the relation: $R_{ij} := R^k_{ikj} = \Omega^k_i(e_k, e_j)$ such that:

$$\begin{cases} R_{00} = -\mathcal{E} - 2\tilde{\mathcal{E}} \\ R_{01} = -2\mathcal{H} \\ R_{11} = \mathcal{E} + 2\tilde{\mathcal{F}} \\ R_{12} = R_{13} = 0 = R_{23} \\ R_{22} = R_{33} = \mathcal{F} + \tilde{\mathcal{E}} + \tilde{\mathcal{F}} \end{cases} \implies R = -2(\mathcal{E} + \mathcal{F}) - 4(\tilde{\mathcal{E}} + \tilde{\mathcal{F}}). \quad (2.19)$$

Finally, we get for the Einstein tensor:

$$\begin{cases} G^0_0 = \mathcal{F} + 2\tilde{\mathcal{F}} = \frac{1-f(r)-rf'(r)}{r^2} \\ G^0_1 = -2\mathcal{H} = 0 \\ G^0_2 = G^0_3 = G^1_2 = G^1_3 = G^2_3 = 0 \\ G^1_1 = \mathcal{F} + 2\tilde{\mathcal{E}} = \frac{1-f(r)-rf'(r)}{r^2} \\ G^2_2 = G^3_3 = \mathcal{E} + \tilde{\mathcal{E}} + \tilde{\mathcal{F}} = -\frac{f''(r)}{2} - \frac{f'(r)}{r} \end{cases} \quad (2.20)$$

This is indeed a general result, which does not depend on the choice of the basis. In general, for practicality, we will consider the metric's components to be: $g_{00} = f(r)$, $g_{11} = -1/f(r)$, $g_{22} = -r^2$, $g_{33} = -r^2 \sin^2 \vartheta$.

Let us finally conclude with a remark about the solutions of EFE, given the special

form of the Einstein tensor (2.20). We see that $G^\mu{}_\nu$ has a linear dependence on the metric's components and its derivatives, therefore if we consider $g_{\mu\nu}^{f_1}$ and $g_{\mu\nu}^{f_2}$ to be solutions of (2) in terms of $f_1(r)$ and $f_2(r)$ respectively, then $g_{\mu\nu}^{f_1+f_2} = g_{\mu\nu}^{f_1} + g_{\mu\nu}^{f_2}$ will solve (2) with $T_{\mu\nu}^{f_1+f_2} = T_{\mu\nu}^{f_1} + T_{\mu\nu}^{f_2}$.

2.2.1 Vacuum Solutions

Let us now consider the EFE (2), we call vacuum solutions those solution obtained setting the energy-momentum tensor to zero: $G_{\mu\nu} = \Lambda g_{\mu\nu}$. Raising the indexes we get $G^\mu{}_\nu = \Lambda \delta^\mu{}_\nu$ therefore plugging in the results of the previous section we get the system of equations:

$$\begin{cases} -\frac{f(r) + rf'(r) - 1}{r^2} = \Lambda \\ -\frac{f''(r)}{2} - \frac{f'(r)}{r} = \Lambda \end{cases} \implies \frac{r^2}{2}f''(r) - f(r) + 1 = 0. \quad (2.21)$$

The homogeneous ordinary differential equation can be solved with the ansatz $f(r) \propto r^\alpha$, and a particular solution is just $f = 1$. Thus, we get:

$$f(r) = 1 + \frac{A}{r} + Br^2, \quad (2.22)$$

where A and B are two integration constants. From the final remark of the previous section, we can clearly see that this solution can be thought as the superposition of $f_1(r) = 1 + \frac{A}{r}$ and $f_2(r) = 1 + Br^2$. In fact, integrating the first equation of the system (2.21):

$$\frac{[r(f(r) - 1)]'}{r^2} = -\Lambda \implies f(r) = 1 + \frac{C}{r} - \frac{\Lambda}{3}r^2. \quad (2.23)$$

Thus we see that $f_1(r)$ is obtained setting $\Lambda = 0$, and $f_2(r)$ setting the integration constant $C = 0$.

In particular, there exist two known classes of these solutions, which we can write in static coordinates:

$$\begin{cases} f_1(r) = 1 - \frac{2m}{r} & \text{Schwarzschild} \\ f_2(r) = 1 - \frac{\Lambda}{3}r^2 & \text{deSitter} \end{cases}. \quad (2.24)$$

We can take the superposed solution (2.22) to be:

$$f(r) = 1 - \frac{2m}{r} - \frac{\Lambda}{3}r^2 \quad \text{Schwarzschild - deSitter}. \quad (2.25)$$

We recall that Schwarzschild spacetime is the only spherically symmetric vacuum solutions of EFE with vanishing cosmological constant, and it describes the field outside a spherically symmetric body of mass m , placed at the origin of the coordinates; it is used in particular to model chargeless and non-rotating black holes.

De Sitter spacetime, instead, is the only maximally symmetric vacuum solution of

EFE with positive cosmological constant, usually employed to model an expanding universe.

Let us now comment on the functional form of SdS metric (2.25). Since we can think of Schwarzschild-de Sitter (SdS) spacetime as the geometry obtained placing a black hole of mass m in an otherwise de Sitter universe, this means that this solution possesses both the Schwarzschild black hole horizon and the de Sitter cosmological horizon.

We recall that, in static coordinates, an event horizon corresponds to the Killing horizon, i.e. a region of \mathcal{M} where the timelike Killing vector $K = \partial_t$ becomes null: $g(K, K) = g_{00} = f(r) \equiv 0$:

$$1 - \frac{2m}{r} - \frac{\Lambda}{3}r^2 = 0 \Leftrightarrow r^3 + \frac{3}{\Lambda}(2m - r) = 0. \quad (2.26)$$

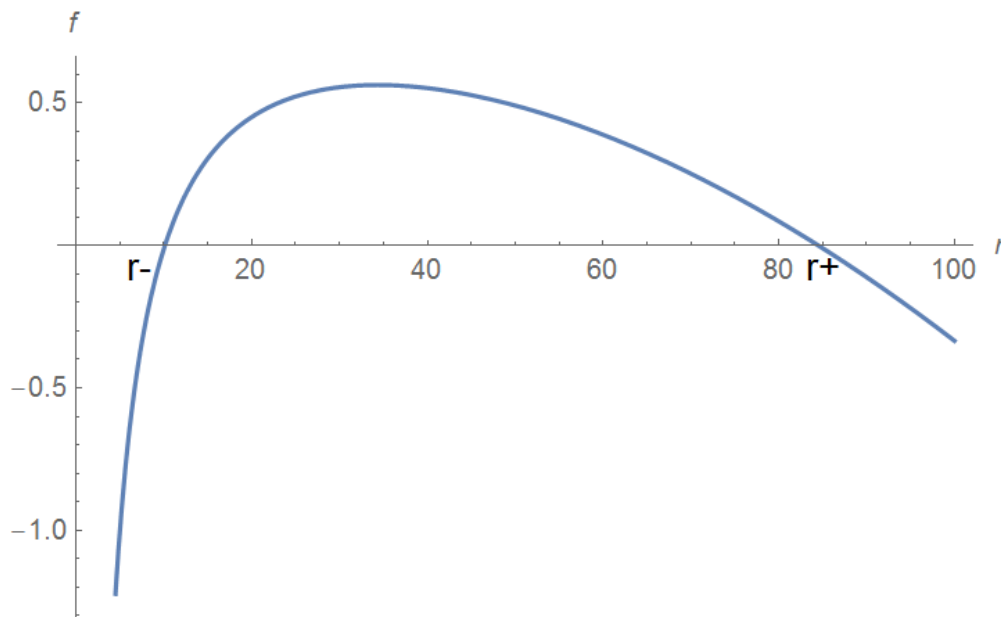
It is possible to show that if $9\Lambda m^2 < 1$ there are two positive zeros corresponding to the horizons, moreover the black hole horizon is larger than in a pure Schwarzschild spacetime, while the cosmological horizon is smaller than in a pure de Sitter spacetime. However, the interpretation of the horizons is the same as in pure geometries: the black hole horizon is a future horizon while the cosmological horizon a past one, where future and past refer to the light cones of any observer.

For our purposes we will always consider scenarios in between the two horizons, far from the zeros of $f(r)$.

To get some intuition on the scales, let us consider a mass of $10^{11}M_{\odot}$, which means $m = 0.5 \times 10^{-2}pc$, and for the cosmological constant $\Lambda = 10^{-13}kpc^{-2}$. For pure geometries we would have $r_- \equiv r_S := 2m = 10^{-2}pc$ and $r_+ \equiv r_{dS} := \sqrt{3/\Lambda} = 5 \times 10^6kpc$, we can assume this values to hold also in SdS spacetime given that $\Lambda m^2 = 0.25 \times 10^{-23}$.

To conclude we show a plot of $f(r)$, where the parameters are chosen to better visualize the functional behavior, and the units are arbitrary.

FIGURE 2.1: SdS metric component $g_{00} = f(r)$.



2.3 Generalized Birkhoff's Theorem with $\Lambda > 0$

Theorem 2. *The only locally spherically symmetric solutions of $G_{\mu\nu} = \Lambda g_{\mu\nu}$ are locally isometric either to one of the Schwarzschild-de Sitter family of solutions or to Nariai spacetime.*

Before proceeding with the proof, let us first clarify the statement above. Two solutions g and g' , on manifolds \mathcal{M} and \mathcal{M}' , are locally isometric if there exist a local diffeomorphism $\phi : \mathcal{M} \rightarrow \mathcal{M}'$ such that: $g'(\phi_*v, \phi_*w) = g(v, w)$ for all $v, w \in \mathcal{T}_p(\mathcal{M}')$, and all $p \in \mathcal{M}'$. In practice we will need to find a change of coordinates such that the notion of distance between points is locally preserved.

Proof. Let us consider \mathcal{U} a subset of \mathcal{M} in which the metric takes the form (2.7). With the formalism introduced in the previous section, it is possible to write the EFE in terms of the functions (2.17), that take now take the form:

$$\begin{cases} \mathcal{E} = e^{-2a}(\dot{b}^2 - \dot{a}\dot{b} + \ddot{b}) - e^{-2b}(a'^2 - a'b' + a'') \\ \tilde{\mathcal{E}} = \frac{1}{R}e^{-2a}(\ddot{R} - \dot{a}\dot{R}) - \frac{1}{R}e^{-2b}a'R' \\ \mathcal{H} = \frac{1}{R}e^{-a-b}(\dot{R}' - a'\dot{R} - \dot{b}R') \\ \mathcal{F} = \frac{1}{R^2}(1 - R'^2e^{-2b} + \dot{R}^2e^{-2a}) \\ \tilde{\mathcal{F}} = \frac{1}{R}e^{-2a}\dot{b}\dot{R} + \frac{1}{R}e^{-2b}(b'R' - R'') \end{cases} \quad (2.27)$$

Where dots denote derivatives with respect to t and primes derivatives with respect to r .

We now state that a local solution depends on the nature of the hypersurfaces $\Sigma := \{R(t, r) = \text{constant}\}$ in some open neighborhood $\mathcal{U} \subset \mathcal{M}$. First of all, let us recall how it is possible to distinguish any vector X of a manifold based on the length:

- if $g(X, X) > 0$ we say that X is timelike;
- if $g(X, X) < 0$ we say that X is spacelike;
- if $g(X, X) = 0$ we say that X is lightlike.

As a consequence, one possible classification of a 3 dimensional hypersurface is:

- Σ is timelike if the induced metric $g|_{T_x\Sigma}$ has signature $(+--)$ and thus is Lorentzian;
- Σ is spacelike if the induced metric $g|_{T_x\Sigma}$ is negative-definite;
- Σ is lightlike if the induced metric $g|_{T_x\Sigma}$ is degenerate.

Let us now consider each case:

- (i) Σ is timelike in \mathcal{U} .

To see the implications of this assumption let us consider $dR = \dot{R}dt + R'dr$ such that $R' \neq 0$ in \mathcal{U} . This allows us to perform a change of coordinate such that

the metric (2.7) takes the form $ds^2 = Adt^2 + 2Bdt dR - CdR^2 - R^2d\Omega^2$. On Σ , by definition, $dR = 0$ and indeed the induced metric has signature $(+--)$. Hence we can choose $R(t, r) = r$ and (2.27) becomes:

$$\left\{ \begin{array}{l} \mathcal{E} = e^{-2a}(\dot{b}^2 - \dot{a}\dot{b} + \ddot{b}) - e^{-2b}(a'^2 - a'b' + a'') \\ \tilde{\mathcal{E}} = -\frac{a'}{r}e^{-2b} \\ \mathcal{H} = -\frac{\dot{b}}{r}e^{-a-b} \\ \mathcal{F} = \frac{1}{r^2}(1 - e^{-2b}) \\ \tilde{\mathcal{F}} = \frac{b'}{r}e^{-2b} \end{array} \right. . \quad (2.28)$$

From the EFE we get:

$$G^0_1 = -2\mathcal{H} = 0 \implies \dot{b} = 0 \implies b = b(r) \quad (2.29)$$

$$G^0_0 - G^1_1 = 2(\tilde{\mathcal{F}} - \tilde{\mathcal{E}}) = 0 \implies b' + a' = 0 \implies a = a(r) = -b(r). \quad (2.30)$$

Where in the last equation we have considered a new time coordinate t such that the arbitrary integration function is set to zero. The system (2.28) becomes now:

$$\left\{ \begin{array}{l} \mathcal{E} = -e^{2a}(2a'^2 + a'') \\ \tilde{\mathcal{E}} = \tilde{\mathcal{F}} = -\frac{a'}{r}e^{2a} \\ \mathcal{F} = \frac{1}{r^2}(1 - e^{2a}) \end{array} \right. . \quad (2.31)$$

The remaining nontrivial EFE gives:

$$G^0_0 = \mathcal{F} + 2\tilde{\mathcal{F}} = \Lambda \implies \frac{1}{r^2}(1 - e^{2a}) - 2\frac{a'}{r}e^{2a} = \Lambda. \quad (2.32)$$

This equation can be rewritten as:

$$1 - (re^{2a})' = \Lambda r^2 \Leftrightarrow \left[r(1 - e^{2a}) - \frac{\Lambda}{3}r^3 \right]' = 0. \quad (2.33)$$

We can integrate this and renaming the arbitrary integration constant we get:

$$r(1 - e^{2a}) - \frac{\Lambda}{3}r^3 = 2m \implies e^{2a} = 1 - \frac{2m}{r} - \frac{\Lambda}{3}r^2. \quad (2.34)$$

Which gives exactly the SdS solution, in static coordinates, between the two horizons.

(ii) Σ is spacelike in \mathcal{U} .

In this case, repeating the argument of the previous point, we can choose

$R(t, r) = t$ and (2.27) becomes:

$$\begin{cases} \mathcal{E} = e^{-2a}(\dot{b}^2 - \dot{a}\dot{b} + \ddot{b}) - e^{-2b}(a'^2 - a'b' + a'') \\ \tilde{\mathcal{E}} = -\frac{\dot{a}}{t}e^{-2a} \\ \mathcal{H} = -\frac{a'}{t}e^{-a-b} \\ \mathcal{F} = \frac{1}{t^2}(1 + e^{-2a}) \\ \tilde{\mathcal{F}} = \frac{\dot{b}}{t}e^{-2a} \end{cases} . \quad (2.35)$$

From the EFE we get:

$$G^0_1 = -2\mathcal{H} = 0 \implies a' = 0 \implies a = a(t) \quad (2.36)$$

$$G^0_0 - G^1_1 = 2(\tilde{\mathcal{F}} - \tilde{\mathcal{E}}) = 0 \implies \dot{b} + \dot{a} = 0 \implies b = b(t) = -a(t). \quad (2.37)$$

Where in the last equation we have considered a new spatial coordinate r such that the arbitrary integration function is set to zero. The system (2.35) becomes now:

$$\begin{cases} \mathcal{E} = e^{2b}(2\dot{b}^2 + \ddot{b}) \\ \tilde{\mathcal{E}} = \tilde{\mathcal{F}} = \frac{\dot{b}}{t}e^{2b} \\ \mathcal{F} = \frac{1}{t^2}(1 + e^{2b}). \end{cases} \quad (2.38)$$

The remaining nontrivial EFE gives:

$$G^0_0 = \mathcal{F} + 2\tilde{\mathcal{F}} = \Lambda \implies \frac{1}{t^2}(1 + e^{2b}) + 2\frac{\dot{b}}{t}e^{2b} = \Lambda. \quad (2.39)$$

This equation can be rewritten as:

$$1 + \frac{d}{dt}(te^{2b}) = \Lambda t^2 \Leftrightarrow \frac{d}{dt}\left[t(1 + e^{2b}) - \frac{\Lambda}{3}t^3\right] = 0. \quad (2.40)$$

We can integrate this and renaming the arbitrary integration constant we get:

$$t(1 + e^{2b}) - \frac{\Lambda}{3}t^3 = 2m \implies e^{2b} = -1 + \frac{2m}{t} + \frac{\Lambda}{3}t^2 \quad (2.41)$$

Which is the SdS solution outside the horizons.

(iii) Σ is lightlike in \mathcal{U} .

In this case we can choose either $R(t, r) = t - r$ or $R(t, r) = R$, where R is a constant. It can be shown that only the latter option is compatible with the EFE. In this case, repeating the usual procedure, we find the only nontrivial equation:

$$e^{-2a}(\dot{b}^2 - \dot{a}\dot{b} + \ddot{b}) - e^{-2b}(a'^2 - a'b' + a'') = \Lambda = \frac{1}{R^2}. \quad (2.42)$$

Since in \mathcal{U} $R(t, r) = R$ holds, it is always possible to invert locally such relation to get $t = t(r, R)$ and therefore $a = a(r, R)$. We can then perform a change of time coordinate in order to set $a = 0$ on the line $R(t, r) = R$. In this way, we are left with the equation:

$$\dot{b}^2 - \dot{a}\dot{b} + \ddot{b} = \frac{1}{R^2} \quad (2.43)$$

If we now set $B = e^b$ we get that such equation becomes:

$$\frac{\ddot{B}}{B} = \frac{1}{R^2}. \quad (2.44)$$

Which can be solved, again changing coordinates, and it leads to $B(t) = \coth\left(\frac{t}{R}\right)$, known as the Nariai solution:

$$ds^2 = -dt^2 + \coth^2\left(\frac{t}{R}\right) dr^2 + R^2(d\vartheta^2 + \sin^2\vartheta d\varphi^2). \quad (2.45)$$

We have reserved an appendix to describe a bit more this solution. □

2.4 Schwarzschild-de Sitter Circular Geodesics

We now want to study the geodesics of a massive test particle moving in SdS space-time (2.25) with line element:

$$ds^2 = \left(1 - \frac{2m}{r} - \frac{r^2}{l^2}\right) dt^2 - \frac{dr^2}{1 - \frac{2m}{r} - \frac{r^2}{l^2}} - r^2(d\vartheta^2 + \sin^2\vartheta d\varphi^2). \quad (2.46)$$

Where for convenience we have introduced $l^2 = 3/\Lambda$.

Let us consider the particle's trajectory parametrized by its proper time s such that its coordinates are $x^\mu = x^\mu(s) = (t(s), r(s), \vartheta(s), \varphi(s))$.

We recall that, given an affine connection, a geodesic is a curve obtained by the parallel transport of a vector along itself: $\nabla_U U = 0$, in this case such vector is the four-velocity of the test particle: $U = u^\mu \partial_\mu$. In components the geodesic equations are:

$$\begin{cases} \frac{du^\mu}{ds} + \Gamma_{\alpha\beta}^\mu u^\alpha u^\beta = 0 \\ u^\mu = \frac{dx^\mu}{ds} \\ g_{\mu\nu} u^\mu u^\nu = 1 \end{cases}. \quad (2.47)$$

We do not actually need to compute all the Christoffel symbols to obtain the geodesics, in fact looking at the SdS metric, we see that it does not depend on the t and φ coordinates. It is possible to exploit these symmetries considering the following alternative form of the geodesic equations.

$$u_{\alpha,\beta} u^\beta = \frac{1}{2} g_{\sigma\beta,\alpha} u^\sigma u^\beta. \quad (2.48)$$

Hence, we get:

$$\begin{cases} u_{t,\beta}u^\beta = 0 \\ u_{\varphi,\beta}u^\beta = 0 \end{cases} \implies \begin{cases} \frac{du_t}{ds} = 0 \\ \frac{du_\varphi}{ds} = 0 \end{cases} \implies \begin{cases} u_t = \tilde{E} \\ u_\varphi = \tilde{L} \end{cases}. \quad (2.49)$$

Where two first integrals of motion have been introduced, corresponding to the energy and angular momentum per unit mass.

We can already employ the conservation of \tilde{L} to get a further simplification. If we focus our attention on the ϑ component we see that the non-vanishing Christoffel symbols are:

$$\Gamma_{r\vartheta}^\vartheta = \Gamma_{\vartheta r}^\vartheta = \frac{1}{r} \quad \Gamma_{\varphi\varphi}^\vartheta = -\sin\vartheta \cos\vartheta. \quad (2.50)$$

Therefore the geodesic equation reads:

$$\ddot{\vartheta} + \frac{2}{r}\dot{r}\dot{\vartheta} - \sin\vartheta \cos\vartheta \dot{\varphi}^2 = 0, \quad (2.51)$$

where dot derivatives are now derivatives with respect to s .

By symmetry, we know that the test particle's orbit is planar, therefore we are free to take the solution $\vartheta = \frac{\pi}{2}$, rearranging the coordinates so that the trajectory is confined to the equatorial plane.

If we now put everything together, the four-velocity normalization equation in (2.47) gives us the geodesic equation for the last variable:

$$g^{\mu\nu}u_\mu u_\nu = g^{tt}(u_t)^2 + g^{rr}(u_r)^2 + g^{\varphi\varphi}(u_\varphi)^2 = 1 \quad (2.52)$$

$$\iff \frac{\tilde{E}^2}{1 - \frac{2m}{r(s)} - \frac{r^2(s)}{l^2}} - \frac{\dot{r}^2(s)}{1 - \frac{2m}{r(s)} - \frac{r^2(s)}{l^2}} - \frac{\tilde{L}^2}{r^2(s)} = 1. \quad (2.53)$$

Finally we are left with three equations (2.4), (2.49), (2.53) that determine in a unique way the particle's dynamics on the equatorial plane. Moreover, we can recast this equation in a form that allows us to interpret it as a particle moving in a one-dimensional effective potential:

$$\begin{cases} \frac{1}{2}\dot{r}^2 + V_{eff} = \frac{1}{2}\tilde{E}^2 \\ V_{eff}(r) = \left(1/2 - \frac{\tilde{L}^2}{2l^2}\right) + \left(-\frac{m}{r} + \frac{\tilde{L}^2}{2r^2}\right) + \left(-\frac{m\tilde{L}^2}{r^3}\right) - \left(\frac{r^2}{2l^2}\right). \end{cases} \quad (2.54)$$

The terms in the second bracket are well-known classical energies, the first being the attractive Newtonian gravitational potential energy and the second corresponding to the repulsive "centrifugal" potential energy, the third bracket is the Schwarzschild contribution responsible to elliptical orbits' precession. De Sitter contributions appear in the first and last bracket.

Circular geodesics are found as critical points of the effective potential $V'_{eff} = 0$: the minima correspond to stable configuration while the maxima are unstable.

It is actually possible to obtain an analytic expression for the orbits: let us consider $r(s)$ as a function of the angular coordinate $r = r(\varphi(s))$ so that $\dot{r} = \frac{\partial r}{\partial \varphi} \dot{\varphi} = -\frac{\partial r}{\partial \varphi} \frac{\tilde{L}}{r^2}$. We can substitute this expression into equation (2.53) and we get:

$$\frac{1}{f(r(\varphi))} \left\{ \tilde{E}^2 - \left(\frac{\partial r}{\partial \varphi} \right)^2 \left(\frac{\tilde{L}}{r(\varphi)^2} \right)^2 \right\} = 1 + \left(\frac{\tilde{L}}{r(\varphi)} \right)^2, \quad (2.55)$$

where we keep the implicit expression $f(r)$ of (2.25) to avoid cumbersome formulas. Next we note that $\frac{\partial r}{\partial \varphi} = -r^2 \frac{\partial}{\partial \varphi} \left(\frac{1}{r(\varphi)} \right)$ so we can rewrite the equation as:

$$\left(\frac{\tilde{E}}{\tilde{L}} \right)^2 - \left[\frac{\partial}{\partial \varphi} \left(\frac{1}{r(\varphi)} \right) \right]^2 = \left[\frac{1}{\tilde{L}^2} + \left(\frac{1}{r(\varphi)} \right)^2 \right] f(r(\varphi)). \quad (2.56)$$

We now derive both sides with respect to φ and we finally get the orbit equation:

$$\frac{\partial^2}{\partial \varphi^2} \left(\frac{1}{r(\varphi)} \right) + \frac{1}{r(\varphi)} = \frac{m}{\tilde{L}^2} + \frac{3m}{r^2(\varphi)} - \frac{r^3(\varphi)}{l^2 \tilde{L}^2}. \quad (2.57)$$

If we want circular geodesics now we just have to plug in a constant value of r : $r(\varphi) = R$ in the last equation:

$$\frac{1}{R} = \frac{m}{\tilde{L}^2} + \frac{3m}{R^2} - \frac{R^3}{l^2 \tilde{L}^2}. \quad (2.58)$$

We can now solve for \tilde{L} and then find the value of \tilde{E} from equation (2.53). Therefore, the circular geodesics equation are solved by:

$$\begin{cases} \tilde{L} = -R \sqrt{\frac{m - R^3/l^2}{R - 3m}} \\ \tilde{E} = \sqrt{\frac{R}{R - 3m} \left(1 - \frac{2m}{R} - \frac{R^2}{l^2} \right)} \end{cases}, \quad (2.59)$$

where the signs have been chosen in a way that $t(s)$ and $\varphi(s)$ are monotonically increasing functions.

Looking at these relations we immediately see that if $\Lambda = 0$ circular geodesics exist for $R > 3m$, while in the general case there is an upper limit given by $R_{max} = (ml^2)^{1/3}$. Therefore outside the range $3m < R < R_{max}$ it is not possible to assign initial conditions that will lead to circular geodesics.

Keeping this in mind, we can now compute the rotation curve as:

$$v_\varphi(R) := R \frac{d\varphi}{ds} = -R \frac{\tilde{L}}{R^2} = \sqrt{\frac{m - \frac{\Lambda}{3} R^3}{R - 3m}}. \quad (2.60)$$

For a galaxy with total mass $m = 10^{11} M_\odot \approx 5 \times 10^{-6} kpc$, we get $R_{max} \approx 0.5 Mpc$. Let us now plot a comparison between the rotation curve (2.60) and the case with

vanishing cosmological constant.

FIGURE 2.2: SdS vs Schwarzschild rotation curves in linear scale.

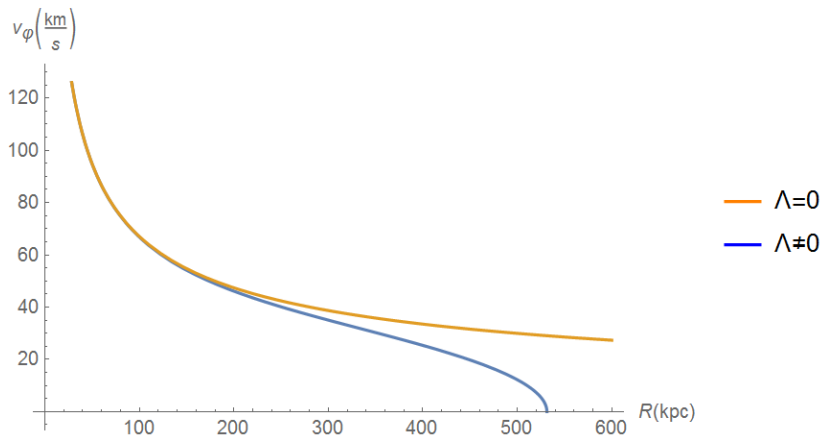
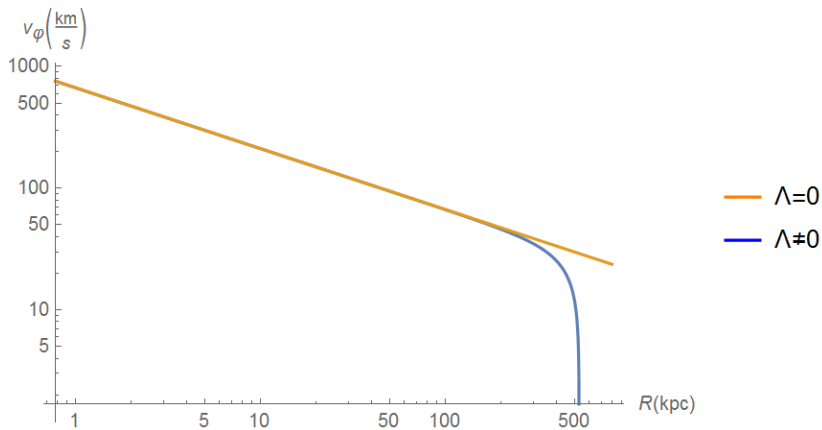


FIGURE 2.3: SdS vs Schwarzschild rotation curves in bilogarithmic scale.



What we can clearly see from the graphs is that the effect of the cosmological constant is to decrease the rotation velocity at a given R with respect to $\Lambda = 0$. To get an estimate of when the cosmological constant becomes relevant, we can compute the radius at which the rotation curve changes concavity R_{flex} . To do so we differentiate twice (2.60) and we set it to zero. After some calculations we find: $R_{flex} = 2^{-2/3}R_{max} \approx 0.3Mpc$.

We can conclude that already in this toy model the cosmological constant has an impact, the extent of which is more relevant at large scales, above roughly $300kpc$. Moreover, this first analysis did not produce flat rotation curve, meaning that we will need to take into account the dark matter contribution in a different way.

2.5 Schwarzschild-de Sitter solution in Conformally Flat Coordinates

We will now repeat the same analysis but we will investigate the SdS spacetime in another coordinate frame, to better take into account the expansion of the Universe.

Let us start by recalling that the static de Sitter metric (2.24):

$$ds^2 = \left(1 - \frac{r^2}{l^2}\right) dt^2 - \frac{dr^2}{1 - \frac{r^2}{l^2}} - r^2 d\Omega^2 \quad (2.61)$$

can be recast in conformally flat coordinates:

$$ds^2 = \frac{l^2}{\eta^2} (d\eta^2 - d\varrho^2 - \varrho^2 d\Omega^2), \quad (2.62)$$

where $\eta < 0$, $\varrho \geq 0$ and $l^{-2} = \frac{\Lambda}{3}$.

We now want to work out explicitly the coordinate transformation:

$$\begin{pmatrix} t \\ r \\ \vartheta \\ \varphi \end{pmatrix} \rightarrow \begin{pmatrix} \eta \\ \varrho \\ \vartheta \\ \varphi \end{pmatrix} \quad (2.63)$$

that leads to (2.62).

Since the angular coordinates are mapped into themselves, we can immediately find:

$$l^2 \frac{\varrho^2}{\eta^2} = r^2 \implies \varrho = -\eta \frac{r}{l} \quad (2.64)$$

Differentiating both sides and plugging it in the expression for the invariant interval in the new coordinates we get:

$$ds^2 + r^2 d\Omega^2 = \frac{l^2}{\eta^2} d\eta^2 - \frac{1}{\eta^2} (\eta^2 dr^2 + d\eta^2 r^2 + 2\eta r d\eta dr) \quad (2.65)$$

$$= \left(\frac{d\eta}{\eta}\right)^2 (l^2 - r^2) - dr^2 - 2\frac{r}{\eta} d\eta dr. \quad (2.66)$$

If we now set:

$$\frac{d\eta}{\eta} = a dt + b dr \quad (2.67)$$

The coefficients a and b have to satisfy the following system of equations in order to reproduce the invariant interval in the original coordinates:

$$\begin{cases} a^2(l^2 - r^2) = \left(1 - \frac{r^2}{l^2}\right) \\ b^2(l^2 - r^2) - 1 - 2br = -\left(1 - \frac{r^2}{l^2}\right)^{-1} \\ 2ab(l^2 - r^2) - 2ar = 0 \end{cases} \quad (2.68)$$

This system is satisfied by:

$$\begin{cases} a = \pm l^{-1} \\ b = \frac{r}{l^2 - r^2} \end{cases}. \quad (2.69)$$

Therefore, we have:

$$\frac{d\eta}{\eta} = \frac{dt}{l} + \frac{r}{l^2 - r^2} dr, \quad (2.70)$$

where the positive root has been chosen, so that $-\eta$ increases when t increases and $\eta \rightarrow 0$ for $t \rightarrow -\infty$. We can rewrite this as:

$$d \left[\ln\left(-\frac{\eta}{l}\right) \right] = d\left(\frac{t}{l}\right) - \frac{1}{2} d \left[\ln\left(\frac{l^2 - r^2}{l^2}\right) \right]. \quad (2.71)$$

If we plug in equation (2.64) for r :

$$d \left[\ln\left(-\frac{\eta}{l}\right) \right] = d\left(\frac{t}{l}\right) - \frac{1}{2} d \left[\ln\left(\frac{l^2 - l^2 \varrho^2 / \eta^2}{l^2}\right) \right]. \quad (2.72)$$

We can integrate this equation and solving for $t = t(\eta, \varrho)$ we find that the transformation (2.62) is realized by:

$$\begin{cases} t(\eta, \varrho) = \frac{l}{2} \ln\left(\frac{\eta^2 - \varrho^2}{l^2}\right) \\ r(\eta, \varrho) = -l \frac{\varrho}{\eta} \end{cases}. \quad (2.73)$$

Where the integration constant has been chosen such that $\eta = -l$ for $r = 0$, $t = 0$, $\varrho = 0$.

The first thing we notice from the form of (2.73) is that this transformation maps the static patch only in a region where $\eta < -\varrho$ is satisfied. Also we have that $t < 0 \Leftrightarrow -\sqrt{l^2 + \varrho^2} < \eta < 0$, and $t \geq 0 \Leftrightarrow \eta \leq -\sqrt{l^2 + \varrho^2}$.

Having now the explicit analytic form of the transformation between the two coordinate frames we can apply this to SdS (2.25) to have a more cosmological based description. In particular, we can apply:

$$\begin{cases} dt = \frac{l}{\eta^2 - \varrho^2} (\eta d\eta - \varrho d\varrho) \\ dr = \frac{l}{\eta} \left(d\varrho - \frac{\varrho}{\eta} d\eta \right) \end{cases} \quad (2.74)$$

to any metric of the form:

$$ds^2 = f(r) dt^2 - \frac{dr}{f(r)} - r^2 d\Omega^2, \quad (2.75)$$

and we would find:

$$\begin{aligned}
 ds^2 = \left(\frac{l}{\eta}\right)^2 \left\{ d\eta^2 \left[f\left(-\frac{\varrho}{\eta}l\right) \left(1 - \frac{\varrho^2}{\eta^2}\right)^{-2} - \frac{\varrho^2}{\eta^2} f\left(-\frac{\varrho}{\eta}l\right)^{-1} \right] \right. \\
 - d\varrho^2 \left[f\left(-\frac{\varrho}{\eta}l\right)^{-1} - \frac{\varrho^2}{\eta^2} f\left(-\frac{\varrho}{\eta}l\right) \left(1 - \frac{\varrho^2}{\eta^2}\right)^{-2} \right] \\
 - 2d\eta d\varrho \left[\frac{\varrho}{\eta} f\left(-\frac{\varrho}{\eta}l\right)^{-1} - \frac{\varrho}{\eta} f\left(-\frac{\varrho}{\eta}l\right) \left(1 - \frac{\varrho^2}{\eta^2}\right)^{-2} \right] \\
 \left. - \varrho^2 d\Omega^2 \right\}. \quad (2.76)
 \end{aligned}$$

In the case of de Sitter spacetime $f = 1 - \rho^2/\eta^2$ and we can see that it correctly reproduces (2.62).

For SdS $f = 1 + 2m\eta/l\rho - \rho^2/\eta^2$; in the next section we will analyze in somewhat more detail this metric.

2.5.1 Spiral Geodesics

We want to repeat the same procedures employed previously, in particular the trajectory of a test particle is now $x^\mu = x^\mu(s) = (\eta(s), \varrho(s), \vartheta(s), \varphi(s))$. Given the symmetry associated to the cyclic variable $\varphi(s)$, we can again restrict our attention to orbits $x^\mu(s) = (\eta(s), \varrho(s), \pi/2, \varphi(s))$. However, the SdS metric is more difficult to analyze in this coordinate frame because there are no other integrals of motion, so the geodesics equations are merely partial differential equations and analytical solutions will not be carried out.

As we are interested in geodesics that maintain fixed the physical distance from the origin, we will transform the circular geodesics found in static SdS (2.59) via (2.73) to get the corresponding orbits in these cosmological coordinates. First of all let us invert the transformation to get $\eta = \eta(t, r)$ and $\varrho = \varrho(t, r)$

$$\begin{cases} \eta(t, r) = -l^2 \frac{e^{t/l}}{\sqrt{l^2 - r^2}} \\ \varrho(t, r) = rl \frac{e^{t/l}}{\sqrt{l^2 - r^2}} \end{cases}. \quad (2.77)$$

We now want to discuss where SdS circular geodesics, with $r(s) = R$, are mapped. Differentiating $\varrho(t, r = R)$ we get:

$$d\varrho = \frac{\varrho}{l} dt. \quad (2.78)$$

For a circular geodesic in static SdS there exists an analytic expression for $t(\varphi)$, in particular:

$$\frac{dt}{ds} = \frac{\partial t}{\partial \varphi} \frac{d\varphi}{ds} \implies \frac{\tilde{E}}{f(R)} = -\frac{\partial t}{\partial \varphi} \frac{\tilde{L}}{R^2}. \quad (2.79)$$

Therefore:

$$dt = \frac{\partial t}{\partial \varphi} d\varphi \implies dt = -\frac{\tilde{E}}{\tilde{L}} \frac{R^2}{f(R)} d\varphi. \quad (2.80)$$

Substituting in (2.78) we get:

$$\frac{d\varrho}{\varrho} = -\frac{\tilde{E}}{\tilde{L}} \frac{R^2}{f(R)} \frac{d\varphi}{l}. \quad (2.81)$$

Finally thanks to (2.59) we get:

$$\varrho(R, \varphi) = \varrho_0 \exp \left\{ \frac{R}{l} \sqrt{\frac{R}{m - \frac{R^3}{l^2}}} \varphi \right\}. \quad (2.82)$$

Hence we can see that to each circular geodesic in the static frame, there corresponds a spiral orbit in the cosmological frame, which is still a geodesic.

It is interesting to compute the displacement after one revolution: $\frac{\Delta \varrho(R, \varphi)}{\varrho_0} := \frac{\varrho(R, \varphi) - \varrho_0}{\varrho_0}$

$$\frac{\Delta \varrho(R, 2\pi)}{\varrho_0} = \exp \left\{ \frac{2\pi R}{l} \sqrt{\frac{R}{m - \frac{R^3}{l^2}}} \right\} - 1 \quad (2.83)$$

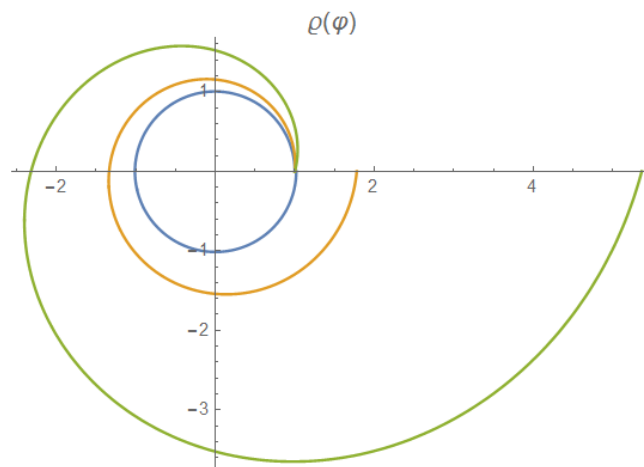
In the following, we show some numerical values of the displacements:

TABLE 2.1: Radial displacement after 2π rotation.

$\frac{\Delta \varrho(R, 2\pi)}{\varrho_0}$	$R = 10kpc$	$R = 0.1Mpc$	$R = 0.2Mpc$	$R = 0.4Mpc$
	0.02	0.8	4	800

And lastly the plots of the orbits for the first three values of R in Table 2.1.

FIGURE 2.4: Spiral geodesics



From these numbers we can readily compute the displacement after n revolutions:

$$\frac{\Delta\varrho(R, 2n\pi)}{\varrho_0} = \left(\frac{\Delta\varrho(R, 2\pi)}{\varrho_0} + 1 \right)^n - 1 \quad (2.84)$$

If we take for instance the value of $R = 10kpc$, we have discussed in the first chapter that, on average, the galactic components at this radius have roughly completed thirty revolutions. This value can be obtained also in the SdS solution, with $v_\varphi(R = 10kpc) \approx 200kms^{-1}$. Since the angular coordinates are mapped into themselves by the transformation (2.62), also the number of revolution is the same. We can therefore compute:

$$\frac{\Delta\varrho(R = 10kpc, 2\pi n = 2\pi 30)}{\varrho_0} = (0.02 + 1)^{30} - 1 \approx 0.8. \quad (2.85)$$

For higher radii SdS does not reproduce flat rotation curves, so we cannot rely on the values of (2.60) to count the number of revolutions and the total displacement. In any case, we can conclude that in this coordinate system the rate of the expansion of the Universe, i.e. the cosmological constant, kicks in much earlier than the static case. However for what concerns the rotation curves, since ds is an invariant and the angular coordinates are mapped into themselves, we get that the rotation velocity is the same; what this cosmological frame adds to the static description is a radial velocity component, which is irrelevant for our problem.

2.6 Rotation Curves seen by a far-away geodesic observer

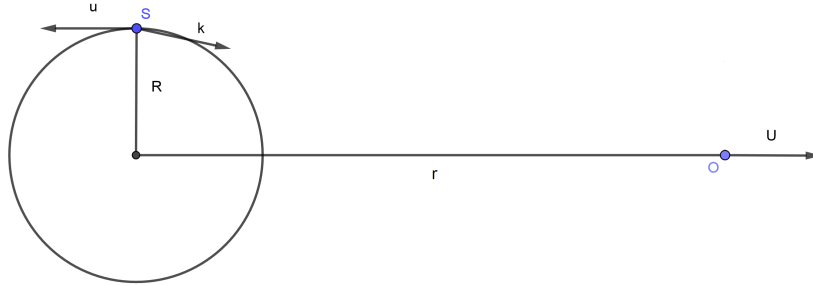
So far we have claimed that the quantity $v_\varphi(R) = R \frac{d\varphi}{ds}$ describes the rotation curve of a galaxy from a geometrical perspective. We are now asking ourselves if this quantity is actually what astronomers measure.

To address this issue we will try to reproduce in our toy model the observation strategy discussed in the first chapter and, since we will deal with covariant quantities, we can just restrict our attention to the static SdS spacetime.

As we said, in this simplified model, we consider the mass of the galaxy centered at the origin of the coordinates, and we now consider a hydrogen atom in a circular geodesic motion around this point. Due to the spin flip transition that occurs in the galactic environment, the hydrogen atom emits a photon that will eventually reach the radio telescope of a far-away observer who, from the redshift measure, will be able to infer the hydrogen velocity.

We will consider the observer to follow a geodesic in the SdS spacetime, far from the center of the galaxy but still within the cosmological horizon. The sketch we will refer to is the following:

FIGURE 2.5: Far-away observer O receiving light from the emitting source S given by the hydrogen atom. The whole dynamics takes place on the equatorial plane.



Let us call ν_S the frequency of the radiation as it is emitted by the hydrogen source, and ν_O the frequency as it reaches the observer. We recall then the definition of the redshift z :

$$1 + z = \frac{\nu_S}{\nu_O} \quad (2.86)$$

For our purposes, we need to rewrite this quantity in a covariant way.

We consider an observer with four-velocity U^μ , and a photon with wave-vector k^μ . The product $U^\mu k_\mu$ is Lorentz invariant, and therefore it has the same value in each reference frame. If we choose in particular the local inertial frame of the observer, $U^\mu k_\mu = U^0 k_0 = E_\gamma$, which is the energy of the photon as it reaches the observer. If we call u^μ the four-velocity of the hydrogen atom, we can then rewrite the redshift z as:

$$1 + z = \frac{u^\mu (k_\mu)_S}{U^\mu (k_\mu)_O}, \quad (2.87)$$

where the subscripts S and O mean that the wave-vector is evaluated respectively at the position of the source (hydrogen atom) or of the observer.

Since the hydrogen atom follows a circular geodesic in static SdS, we already know its four-velocity:

$$\begin{aligned} u^\mu &= \left(\frac{dt}{ds_S}, \frac{dr}{ds_S}, \frac{d\vartheta}{ds_S}, \frac{d\varphi}{ds_S} \right) = \left(\frac{\tilde{E}}{f(R)}, 0, 0, -\frac{\tilde{L}}{R^2} \right) = \\ &= \left[1 - \frac{3m}{R} \right]^{-1/2} \left(1, 0, 0, \frac{1}{R} \sqrt{\frac{m}{R} - \frac{R^2}{l^2}} \right). \end{aligned} \quad (2.88)$$

For what concerns the photon, let us consider its trajectory on the equatorial plane parametrized by an affine parameter λ , then we can express its wave-vector as:

$$k^\mu = k^\mu(\lambda) = \left(\frac{dt}{d\lambda}, \frac{dr}{d\lambda}, \frac{d\vartheta}{d\lambda}, \frac{d\varphi}{d\lambda} \right) \equiv (k^0, k^1, 0, k^3). \quad (2.89)$$

Since the photon follows a geodesic in SdS spacetime, from what we have discussed

previously, we know that there are two integrals of motion, namely: $E = k_0$ and $L = k_3$. We also know that the normalization condition for the wave-vector is $k_\mu k^\mu = 0$, as it is a lightlike vector. From this condition, we get:

$$\frac{E^2}{f(r)} - \frac{\dot{r}^2}{f(r)} - \frac{L^2}{r^2} = 0 \implies \dot{r} = \pm |E| \sqrt{1 - \frac{b^2}{r^2} f(r)}, \quad (2.90)$$

where we have defined the impact parameter $b = L/E$. Let us consider $r(\lambda)$ to be a monotonic increasing function and $E > 0$, then we have:

$$k_\mu = E \left(1, -\frac{1}{f(r)} \sqrt{1 - \frac{b^2}{r^2} f(r)}, 0, b \right) \equiv E \kappa_\mu, \quad (2.91)$$

where we have introduced the auxiliary wave-vector κ^μ .

Let us now consider the fact that the observer is so far away ($r(s_O) \gg R, \forall s_O$) that the light emitted by the hydrogen atom travels such a great distance, that it can be approximated to leave tangentially the circular geodesics. This means that, at the source, the radial component of the wave-vector vanishes, i.e.:

$$b = \pm \frac{R}{\sqrt{f(R)}}, \quad (2.92)$$

where the two roots represent the receding and approaching configuration of the hydrogen atom with respect to the observer. To describe the situation in Figure 2.5 we need to take the positive root.

Finally, we find the expression for the wave-vector at the two locations:

$$\begin{cases} (\kappa_\mu)_S = \left(1, 0, 0, \frac{R}{\sqrt{f(R)}} \right) \\ (\kappa_\mu)_O = \left(1, -\frac{1}{f(r)} \sqrt{1 - \left(\frac{R}{r}\right)^2 \frac{f(r)}{f(R)}}, 0, \frac{R}{\sqrt{f(R)}} \right) \end{cases}. \quad (2.93)$$

Let us now specify the geodesic motion of the far-away observer. We want to analyze the case of a radially moving observer in SdS spacetime:

$$U^\mu = \left(\frac{dt}{ds_O}, \frac{dr}{ds_O}, \frac{d\vartheta}{ds_O}, \frac{d\varphi}{ds_O} \right) \equiv (U^0, U^1, 0, 0) = \left(\frac{\tilde{E}}{f(r)}, \sqrt{\tilde{E}^2 - f(r)}, 0, 0 \right), \quad (2.94)$$

where, as usual, we have introduced the first integral of motion $\tilde{E} = U_0$, and we have made use of the normalization condition, assuming also $r(s_O)$ to be a monotonic increasing function.

Let us now compute the redshift (2.87). The numerator reads:

$$u^\mu (\kappa_\mu)_S = \left[1 - \frac{3m}{R} \right]^{-1/2} \left\{ 1 + \sqrt{\frac{m/R - R^2/l^2}{1 - 2m/R - R^2/l^2}} \right\}, \quad (2.95)$$

while the denominator:

$$\begin{cases} U^\mu(\kappa_\mu)_O = \frac{\tilde{E}}{f(r)} - \frac{\sqrt{\tilde{E}^2 - f(r)}}{f(r)} \sqrt{1 - \left(\frac{R}{r}\right)^2 \frac{f(r)}{f(R)}} \\ f(r) = 1 - 2m/r - r^2/l^2 \\ f(R) = 1 - 2m/R - R^2/l^2 \end{cases} \quad (2.96)$$

We now want to make some approximations, coherently with the scales we are dealing with. As usual we will consider the values $m \approx 5 \times 10^{-6} kpc$, and $l^2 = 2.5 \times 10^{13} kpc^2$.

For the motion of the source we recall that circular geodesics in SdS spacetime are possible in the range $3m < R < R_{max} = (ml^2)^{1/3} \approx 0.5 Mpc$, therefore we can assume this scale interval to represent the order of magnitude of R . For the motion of the observer, instead it is necessary to make further considerations.

From equation (2.94):

$$\begin{cases} \left(\frac{dr}{ds_O}\right)^2 + f(r) = \tilde{E}^2 \\ \tilde{E}^2 \geq f(r) \\ f(r) = 1 - 2m/r - r^2/l^2 \end{cases} \quad (2.97)$$

we see that it is possible to have a stationary observer, for every time s_O , only if $r(s_O) = r^*$, where r^* is the maximum of $f(r)$, i.e. $f'(r) = 0 \Leftrightarrow r = r^* = (ml^2)^{1/3}$. Since this value is equivalent to R_{max} , we cannot assume this configuration to model the observational strategy we have in mind, and we will need to consider a moving observer.

As we have discussed, SdS spacetime reduces asymptotically to the de Sitter spacetime, which is indeed not flat and has a horizon at $r = r_+ = l$. With this remark, we need to find a compromise between having an observer far from the orbit of the galactic hydrogen atom, but still inside the cosmological horizon.

Let us then consider the initial position of the observer to be $r(s_O = 0) = 10^5 kpc$, if we now assume the energy to be $\tilde{E} = 1$, and we consider the spacetime to be well approximated by de Sitter, equations (2.97) become:

$$\frac{dr}{ds_O} = \frac{r}{l} \implies r(s_O) = r(0)e^{s_O/l}. \quad (2.98)$$

Plugging in numbers, it can be checked that it would take roughly 10^{10} years for this observer to reach the cosmological horizon, which makes this configuration suitable for our scheme.

Assuming this scenario we have $2m \ll r, R \ll l$ and $r \gg R$. With this in mind we will now expand the redshift z (2.87) keeping up to the first order in m/R , R^2/l^2 , r^2/l^2 and R^2/l^2 . Also we will neglect m/r , as we are not interested in Schwarzschild modifications to the de Sitter solution that already well describes the spacetime in which the observer moves.

Starting from the numerator (2.95) we have:

$$u^\mu(\kappa_\mu)_S \approx \left(1 + \frac{3m}{2R}\right) + \sqrt{\frac{m}{R} - \frac{R^2}{l^2}} \left(1 + \frac{5m}{2R} + \frac{R^2}{2l^2}\right), \quad (2.99)$$

and the denominator (2.96) becomes:

$$\begin{cases} U^\mu(\kappa_\mu)_O = \frac{1}{f(r)} - \frac{\sqrt{1-f(r)}}{f(r)} \sqrt{1 - \left(\frac{R}{r}\right)^2 \frac{f(r)}{f(R)}} \\ f(r) = 1 - r^2/l^2 \\ f(R) = 1 - 2m/R - R^2/l^2 \end{cases} \quad (2.100)$$

$$\Rightarrow U^\mu(\kappa_\mu)_O \approx \left(1 + \frac{r^2}{l^2}\right) \left\{1 - \frac{r}{l} \left[1 - \frac{1}{2} \left(\frac{R}{r}\right)^2 \left(1 + \frac{r^2}{l^2}\right) \left(1 + \frac{2m}{R} + \frac{R^2}{l^2}\right)\right]\right\}.$$

Thus:

$$1 + z \approx \frac{1 + \frac{3m}{2R} + \sqrt{\frac{m}{R} - \frac{R^2}{l^2}} \left(1 + \frac{5m}{2R} + \frac{R^2}{2l^2}\right)}{\left(1 + \frac{r^2}{l^2}\right) \left\{1 - \frac{r}{l} \left[1 - \frac{1}{2} \left(\frac{R}{r}\right)^2 \left(1 + \frac{r^2}{l^2}\right) \left(1 + \frac{2m}{R} + \frac{R^2}{l^2}\right)\right]\right\}}. \quad (2.101)$$

We can now relate this expression to the velocity that is measured by the observer. If we say that the source moves with velocity $\vec{\beta}$ with respect to the observer, we know that from the relativistic Doppler effect we have (see J. Plebanski, 2006):

$$v_S = (1 - \beta^2)^{-1/2} (v_O - \vec{\beta} \cdot \vec{k}) = v_O \sqrt{\frac{1 + \beta}{1 - \beta}} \Rightarrow 1 + z = \sqrt{\frac{1 + \beta}{1 - \beta}}, \quad (2.102)$$

Where we have defined $\beta := \|\vec{\beta}\|$, and we have considered that in our approximation $\vec{\beta}$ is antiparallel to the direction of propagation of the light. Since $\beta \ll 1$, at the first order we find:

$$\beta \approx z \approx \frac{1 + \frac{3m}{2R} + \sqrt{\frac{m}{R} - \frac{R^2}{l^2}} \left(1 + \frac{5m}{2R} + \frac{R^2}{2l^2}\right)}{\left(1 + \frac{r^2}{l^2}\right) \left\{1 - \frac{r}{l} \left[1 - \frac{1}{2} \left(\frac{R}{r}\right)^2 \left(1 + \frac{r^2}{l^2}\right) \left(1 + \frac{2m}{R} + \frac{R^2}{l^2}\right)\right]\right\}} - 1. \quad (2.103)$$

If we now compare this formula with the expression given by (2.60), we see that they coincide with one another at the lowest order in the expansion we have described:

$$\beta \approx \sqrt{\frac{m}{R} - \frac{R^2}{l^2}} \quad (2.104)$$

Therefore, we can conclude that the theoretical rotation velocity agrees with what astronomers can access experimentally. In the following, we will assume this conclusion valid even for other galactic models, as we always consider our observations to take place outside the boundary of the external galaxy.

Chapter 3

Spherically Symmetric Inhomogeneous Solutions of Einstein Field Equations with $\Lambda > 0$

This chapter aims to explore a reasonable description of the galaxy based on the astronomical picture we presented in the first chapter, always in the light of the Λ CDM Model.

The main issue of the SdS model is that it considers the test particles' motion to take place in vacuum and not within the galaxy itself; as a consequence to obtain a more realistic model we need to better specify the geometry of the spacetime where we want to investigate the circular geodesics. From what we have learned from our toy model, we expect an eventual effect of the cosmological constant to be present only beyond the scales of the galactic disk; hence we need to focus our attention to the dark halo, at scales where the luminous contribution is neglectable.

In the following we will study EFE (2) with positive cosmological constant, and with the energy-momentum tensor that refers to the dark halo. We will always keep the simplifying hypothesis of spherical symmetry to work with exact solutions.

We are now going to start the chapter with a discussion on the implications of such a hypothesis on inhomogeneous models, and we will then focus on our specific case described by the Lemaître-Tolman model. For this part, given by the first two sections, we will follow faithfully the reference J. Plebanski, 2006.

3.1 Spherically symmetric inhomogeneous models

Let us consider a spherically symmetric spacetime in which the source in Einstein's equations is a perfect fluid. We have shown that it is possible to introduce suitable coordinates such that the metric tensor takes the form (2.7):

$$ds^2 = e^{2a(t,r)} dt^2 - e^{2b(t,r)} dr^2 - R^2(t,r) d\Omega^2, \quad (3.1)$$

we can also work in comoving coordinates such that the velocity field is $u^\mu = e^{-a} \delta^\mu_0$. This choice is often referred to as comoving-synchronous coordinates (for further reference see J. Plebanski, 2006).

It is important to remark that the area of the surface $\{t = \text{constant}, r = \text{constant}\}$ is given by $4\pi R^2$, therefore the quantity associated to physical separations in this spacetime, the so called areal distance, is given by $R(t, r)$ which is a function of the

spacetime coordinates themselves.

The EFE for this metric with the cosmological constant and the source taken into account are:

$$\begin{cases} G^\mu{}_\nu = \Lambda \delta^\mu{}_\nu + 8\pi T^\mu{}_\nu \\ T^\mu{}_\nu = (P + \rho)u^\mu u_\nu - P\delta^\mu{}_\nu \\ u^\mu = e^{-a}\delta^\mu{}_0 \end{cases} \quad (3.2)$$

where P is the pressure of the fluid and ρ is its energy density, which in this coordinates is nothing but the mass density.

The Einstein tensor, thanks to (2.27), has the following components:

$$\begin{cases} G^0{}_0 \equiv e^{-2a} \left(\frac{\dot{R}^2}{R^2} + \frac{2\dot{b}\dot{R}}{R} \right) - e^{-2b} \left(2\frac{R''}{R} + \frac{\dot{R}^2}{R^2} - \frac{2b'R'}{R} \right) + \frac{1}{R^2} = \Lambda + 8\pi\rho \\ G^1{}_0 \equiv e^{-2b} \left(2\frac{\dot{R}'}{R} - \frac{2\dot{b}R'}{R} - \frac{2\dot{R}a'}{R} \right) = 0 \\ G^1{}_1 \equiv e^{-2a} \left(2\frac{\ddot{R}}{R} + \frac{\dot{R}^2}{R^2} - \frac{2\dot{R}\dot{a}}{R} \right) - e^{-2b} \left(\frac{R'^2}{R^2} + \frac{2R'a'}{R} \right) + \frac{1}{R^2} = \Lambda - 8\pi P \end{cases} \quad (3.3)$$

As usual we denote derivatives with respect to t with a dot and derivatives with respect to r with a prime, also we will always consider the case where the derivatives of $R(t, r)$ are non-vanishing. The remaining equations for $G^2{}_2 = G^3{}_3$ can be obtained from the Bianchi's identities $G^{\mu\nu}{}_{;\mu} = G^\mu{}_{\nu;\mu} = 0$ therefore we will not write them down explicitly.

We can rewrite the first equation multiplying both sides by R^2R' .

$$\left[R + e^{-2a}R\dot{R}^2 - e^{-2b}RR'^2 - \frac{\Lambda}{3}R^3 \right]' - R \left[e^{-2a}\dot{R}^2 \right]' + 2e^{-2a}\dot{b}R\dot{R}R' = 8\pi R^2R'\rho, \quad (3.4)$$

moreover, taking into account the second EFE we get:

$$\left[R + e^{-2a}R\dot{R}^2 - e^{-2b}RR'^2 - \frac{\Lambda}{3}R^3 \right]' = 8\pi R^2R'\rho. \quad (3.5)$$

We can treat the third equation in a similar fashion, multiplying both sides by $R^2\dot{R}$. We finally get:

$$\frac{\partial}{\partial t} \left(R + e^{-2a}R\dot{R}^2 - e^{-2b}RR'^2 - \frac{\Lambda}{3}R^3 \right) = -8\pi R^2\dot{R}P. \quad (3.6)$$

We can now recognize that the expression in the brackets has the same behavior of a mass:

$$\mathcal{M}(t, r) := \frac{R + e^{-2a}R\dot{R}^2 - e^{-2b}RR'^2 - \frac{\Lambda}{3}R^3}{2}. \quad (3.7)$$

On a hypersurface of constant time $\{t = t_0\}$ we find the familiar expression:

$$d\mathcal{M} \equiv \mathcal{M}'dr + \dot{\mathcal{M}}dt \implies \mathcal{M}'(t_0, r) = 4\pi R(t_0, r)^2R'(t_0, r)\rho(t_0, r). \quad (3.8)$$

Equation (3.6) instead can be interpreted as the energy conservation equation.

To proceed and solve the EFE, it is necessary to assume an equation of state for the source. If we think about the physical model of the galaxy that we have laid out, we have a reasonable assumption: as our description is based on the Λ CDM Model, it suggests us to assume $P = 0$, since the dark halo is made of cold dark matter particles, i.e. non-relativistic.

This particular solution of the spherically symmetric inhomogeneous model will be presented in the next section.

3.2 The Lemaître-Tolman Solution

Let us consider a perfect fluid with negligible pressure, in this case, the evolution of the system is driven by gravitation only and the particles of the fluid follow timelike geodesics. As the acceleration du^μ/ds must be zero, it has to be that $a'(t, r)$ must be zero as well. This gives us the freedom to reparametrize the time coordinate such that $a(t) = 0$.

Thus the EFE (3.2) become now:

$$\begin{cases} G^\mu{}_\nu = \Lambda\delta^\mu{}_\nu + 8\pi T^\mu{}_\nu \\ T^\mu{}_\nu = \rho u^\mu u_\nu \\ u^\mu = \delta^\mu{}_0 \end{cases} . \quad (3.9)$$

Accordingly the second equation in (3.3) now gives:

$$\frac{\partial}{\partial t} \left(e^{-b(t,r)} R' \right) = 0 \quad (3.10)$$

which can be integrated to find:

$$e^{2b(t,r)} = \frac{R'^2(t,r)}{1 + 2E(r)}, \quad (3.11)$$

where we have introduced the integration function $E(r)$, that has to satisfy the inequality $E(r) > -1/2$ for all r .

Now looking at the third equation in (3.3) we obtain:

$$2\frac{\ddot{R}}{R} + \frac{\dot{R}^2 - 2E}{R^2} - \Lambda = 0. \quad (3.12)$$

Multiplying both sides by $R^2\dot{R}$ it becomes:

$$\frac{\partial}{\partial t} \left[R \left(\dot{R}^2 - 2E - \frac{\Lambda}{3} R^2 \right) \right] = 0 \implies \dot{R}^2 = 2\frac{M(r)}{R} + \frac{R^2}{l^2} + 2E(r) \quad (3.13)$$

where in this case the integration function is $2M(r)$, and again we introduced $l^{-2} = \Lambda/3$.

From this equation, we can also read an interpretation for the integration functions. In fact, for vanishing cosmological constant this equation is formally identical to the Newtonian equation of radial motion in a Coulomb potential, therefore in this

analogy $M(r)$ plays the role of the active gravitational mass within a $\{r = \text{constant}\}$ shell, and $E(r)$ the total energy within the same shell.

Finally the first equation in (3.3) tells us $\mathcal{M} = M$:

$$4\pi\rho = \frac{M'}{R^2 R'} \quad (3.14)$$

where we can see that there exist two singularities: either $R = 0 \neq M'$ or $R' = 0 \neq M'$. The first possibility is called the Big Bang singularity, which is unavoidable for $\Lambda = 0$, and the second possibility is called shell-crossing singularity which can be avoided with tuned choices of the integration functions. For our purposes, we will not have to deal with these delicate situations.

Ultimately, the solution of EFE that goes by the name Lemaître-Tolman (LT) solution is

$$ds^2 = dt^2 - \frac{R^2}{1 + 2E(r)} dr^2 - R^2(t, r)(d\vartheta^2 - \sin^2 \vartheta d\varphi^2) \quad (3.15)$$

The function $R(t, r)$ is determined by solving (3.13), but we note that explicit solutions can be written in terms of elementary functions only in the case $\Lambda = 0$. We will now display them to gain some intuition.

$$\text{if } E(r) < 0 \implies \begin{cases} R(t, r) = -\frac{M}{2E}(1 - \cos \zeta) \\ \zeta - \sin \zeta = \frac{(-2E)^{3/2}}{M}(t - t_B(r)) \end{cases} \quad (3.16)$$

$$\text{if } E(r) = 0 \implies R(t, r) = \left[\frac{9}{2} M(r) (t - t_B(r))^2 \right]^{1/3} \quad (3.17)$$

$$\text{if } E(r) > 0 \implies \begin{cases} R(t, r) = \frac{M}{2E}(\cosh \zeta - 1) \\ \sinh \zeta - \zeta = \frac{(2E)^{3/2}}{M}(t - t_B(r)) \end{cases} \quad (3.18)$$

where a further integration function has been defined $t_B(r)$, usually called the bang-time function.

Let us now discuss some limits of the LT solution.

First of all from equation (3.14) we see that $M'(r) = 0$ implies that the model becomes vacuum and since it is spherically symmetric we know from Birkhoff's theorem that the solution must reduce to SdS spacetime, however it is not straightforward to check it explicitly in these comoving-synchronous coordinates.

The other limit we want to discuss is the Friedmann solution, i.e. when the inhomogeneities are lost and we recover the spherically symmetric homogeneous solution that satisfies the Cosmological Principle. This is achieved by

$$M(r) = M_0 r^3, \quad E(r) = -\frac{1}{2} k r^2, \quad t_B(r) = \text{constant}. \quad (3.19)$$

We can in fact define $R(t, r) \equiv a(t)\mathfrak{r}(r)$ and noticing that local transformations of the type $r = f(r')$ do not change the form of the solution we can choose $\mathfrak{r} = r$. The

solution reduces immediately to Friedmann-Lemaître (1.3):

$$ds^2 = dt^2 - a^2(t) \left(\frac{dr^2}{1 - kr^2} - r^2 d\Omega^2 \right). \quad (3.20)$$

Moreover from equations (3.13) and (3.14) we obtain the Friedmann equation for the scale factor:

$$\dot{a}^2 + k = (8\pi\rho + \Lambda) \frac{a^2}{3}. \quad (3.21)$$

Differentiating once more and taking into account the derivative of (3.14) we would then find the other Friedmann equation (1.5).

Before ending the section, we would like to make some additional remarks on the arbitrary functions that we have introduced. The LT model (3.15) is a solution of EFE (3.38) if (3.13) and (3.14) are satisfied, let us see in more detail what is necessary to specify to sufficiently determine a particular spherically symmetric inhomogeneous solution of this form.

We can rewrite (3.12) as:

$$\dot{R}^2 + 2R\ddot{R} - \Lambda R^2 = 2E. \quad (3.22)$$

From (3.13) we can find:

$$\dot{R} = \pm \sqrt{2E + \frac{2M}{R} + \frac{R^2}{l^2}} \implies dt \frac{\dot{R}}{\sqrt{2E + \frac{2M}{R} + \frac{R^2}{l^2}}} = \pm dt. \quad (3.23)$$

Integrating at fixed r we get:

$$t - \int_{R(t_0, r)}^{R(t, r)} \frac{dx}{\sqrt{2E + \frac{2M}{x} + \frac{x^2}{l^2}}} = \pm t_0(r) \equiv \pm t_B(r) \quad (3.24)$$

and from (3.14) we find:

$$m + \int_{R(t, r_0)}^{R(t, r)} 4\pi\rho(t_0, r(x))x^2 dx = M(r) \quad (3.25)$$

where we have introduced the integration constant m as a central mass: we will discuss its interpretation in the next section.

From equations (3.22)(3.24)(3.25) what we see then is that a particular solution is specified if we assign the functions:

$$\{E(r), t_B(r), M(r)\} \quad (3.26)$$

or equivalently

$$\{R(t_0, r), \dot{R}(t_0, r), \rho(t_0, r)\}. \quad (3.27)$$

From the already mentioned local symmetry, we can also fix a gauge, for example with the condition:

$$R(t_0, r) = a(t_0)r \quad (3.28)$$

Therefore, in the end we are left with the choice of two arbitrary functions to specify

a particular solution. However we want to simplify the problem a bit more setting $E(r) = 0$. With this assumption the system is usually called "marginally bound" which means that there are no excesses or defects of energy, and the active gravitational mass that generates the gravitational field is equal to the sum of the masses of the particles that form the gravitating body.

The energy function also has another interpretation, as we could already see from the Friedmann limit: if we slice the spacetime in $\{t = \text{constant}\}$ hypersurface, then $E(r)$ gives a measure of their local curvature. In the case $E(r) = 0$ each of these spaces is topologically flat.

3.3 Curvature Coordinates for the Lemaître-Tolman Solution

Comoving coordinates can be of tricky interpretation; hence we now want to display a change of coordinates that would yield to a more intuitive understanding of this geometry.

Starting from (3.15) we look for a transformation in which $R(t, r)$ becomes the radial coordinate such that the spacetime coordinates $(t, r, \vartheta, \varphi)$ are mapped into $(T, R, \vartheta, \varphi)$. We begin considering that

$$R' dr = dR - \dot{R} dt \quad (3.29)$$

and we set

$$t = f(T, R) \implies dt = f_{,T} dT + f_{,R} dR. \quad (3.30)$$

Where the derivatives with respect to the new coordinates are written as subscripts, not to confuse them with the derivatives with respect to the old coordinates.

Substituting these relations in the LT solution (3.15) leads to:

$$\begin{aligned} ds^2 &= (f_{,T} dT + f_{,R} dR)^2 - \frac{1}{1+2E} [dR - \dot{R} (f_{,T} dT + f_{,R} dR)]^2 + \\ &\quad - R^2 d\Omega^2 \\ &= f_{,T}^2 dT^2 + 2f_{,T} f_{,R} dT dR + f_{,R}^2 dR^2 - \frac{1}{1+2E} [dR (1 - \dot{R} f_{,R}) - \dot{R} f_{,T} dT]^2 + \\ &\quad - R^2 d\Omega^2 \\ &= dT^2 \left(f_{,T}^2 - \frac{1}{1+2E} \dot{R}^2 f_{,T}^2 \right) - dR^2 \left[\frac{1}{1+2E} (1 - \dot{R} f_{,R})^2 - f_{,R}^2 \right] + \\ &\quad + 2dTdR \left[f_{,T} f_{,R} + \frac{1}{1+2E} (1 - \dot{R} f_{,R}) \dot{R} f_{,T} \right] - R^2 d\Omega^2 \end{aligned} \quad (3.31)$$

Where \dot{R} , given by (3.13) is now a function of T and R .
The non-vanishing metric coefficients are therefore:

$$\begin{cases} g_{00}(T, R) = f_{,T}^2 \left(1 - \frac{\dot{R}^2}{1+2E} \right) \\ g_{11}(T, R) = f_{,R}^2 \left(1 - \frac{\dot{R}^2}{1+2E} \right) - \frac{1}{1+2E} + 2f_{,R} \frac{\dot{R}}{1+2E} \\ g_{01}(T, R) = f_{,T} f_{,R} \left(1 - \frac{\dot{R}^2}{1+2E} \right) + f_{,T} \frac{\dot{R}}{1+2E} \\ g_{22}(R) = -R^2 \\ g_{33}(R, \theta) = -R^2 \sin^2 \theta \end{cases} \quad (3.32)$$

Even here we consider the simplifying scenario $E = E(T, R) = 0$, and we additionally request $g_{01} \equiv 0$.

This choice leads to:

$$f_{,R} = -\frac{\dot{R}}{1 - \dot{R}^2} \quad (3.33)$$

which in turn gives:

$$g_{11} = \frac{\dot{R}^2}{1 - \dot{R}^2} - 1 + 2\dot{R} \left(-\frac{\dot{R}}{1 - \dot{R}^2} \right) = -\frac{1}{1 - \dot{R}^2}. \quad (3.34)$$

We arrive then at a solution of the form:

$$ds^2 = f_{,T}^2 (1 - \dot{R}^2) dT^2 - \frac{dR^2}{1 - \dot{R}^2} - R^2 d\Omega^2. \quad (3.35)$$

Which we write in a more compact form:

$$\begin{cases} ds^2 = A(T, R) F(T, R) dT^2 - \frac{dR^2}{A(T, R)} - R^2 d\Omega^2 \\ A(T, R) = 1 - \dot{R}^2(T, R) = 1 - \frac{2M(T, R)}{R^2} - \frac{R^2}{l^2} \\ F(T, R) = f_{,T}^2 \end{cases} \quad (3.36)$$

where (3.13) has been taken into account.

We note that, as long as $A > 0$, T is a time coordinate and it is proportional to the proper time of an observer sitting at fixed R . From the consideration we made at the beginning of the last section, R is the areal radius associated to physical distances, therefore we could say that we have found a LT description in a SdS fashion.

Let us now see how the EFE transform. First of all the metric given by (3.36) leads to

an Einstein tensor with the following mixed components:

$$\begin{cases} G^T_T = \frac{[R(1-A)]_{,R}}{R^2} \\ G^R_T = \frac{A_{,T}}{R} \\ G^T_R = -1 \frac{A_{,T}}{RA^2F} \\ G^R_R = -\frac{A(RF_{,R}/F + 1) + RA_{,R} - 1}{R^2} \equiv G^0_0 - \frac{A}{R} \frac{F_{,R}}{F} \end{cases} . \quad (3.37)$$

In this coordinates the perfect fluid is no longer comoving, therefore the particles will move along timelike geodesics with four-velocity u^μ with non-vanishing spatial components. However the spherical symmetry implies only radial motion such as $u^\mu = (u^T, u^R, 0, 0)$ so that the EFE (3.38) become:

$$\begin{cases} G^\mu_\nu = \Lambda \delta^\mu_\nu + 8\pi T^\mu_\nu \\ T^\mu_\nu = \rho u^\mu u_\nu \\ u^\mu = (u^T, u^R, 0, 0) \end{cases} . \quad (3.38)$$

The first equation gives:

$$[R(1-A)]_{,R} = R^2(\Lambda + 8\pi\rho(T, R)u^T u_T) . \quad (3.39)$$

Integrating on constant time hypersurface, we get:

$$R(1-A) = \frac{R^3}{l^2} + 8\pi \int_{R_0}^R d\tilde{R} \tilde{R}^2 \rho(T, \tilde{R})(u^T u_T)(T, \tilde{R}) + 2m \quad (3.40)$$

where we set the integration function as a constant $2m$. Solving now for A :

$$A \equiv 1 - \frac{2M}{R} - \frac{R^2}{l^2} = 1 - \frac{2}{R} \left(4\pi \int_{R_0}^R d\tilde{R} \tilde{R}^2 \rho u^T u_T \right) - \frac{R^2}{l^2} . \quad (3.41)$$

We find the definition of the mass function in these coordinates, i.e. the equivalent of (3.25):

$$M(T, R) = m + 4\pi \int_{R_0}^R d\tilde{R} \tilde{R}^2 \rho(T, \tilde{R})(u^T u_T)(T, \tilde{R}) . \quad (3.42)$$

Let us now focus on the one-one component of the EFE:

$$-\frac{A}{R} \frac{F_{,R}}{F} + \Lambda + 8\pi T^0_0 = \Lambda + 8\pi T^1_1 \implies \frac{F_{,R}}{F} = 8\pi \frac{R}{A} (T^0_0 - T^1_1) . \quad (3.43)$$

Integrating again on a constant time hypersurface we get:

$$F(T, R) = \exp \left\{ 8\pi \int_{R_0}^R d\tilde{R} \frac{\tilde{R}}{A(T, \tilde{R})} \rho(T, \tilde{R}) (u_T u^T - u_R u^R)(T, \tilde{R}) \right\} . \quad (3.44)$$

The integration function has been set to one and the inhomogeneous dust solution is finally specified.

It is actually possible to exploit some more the LT model to gain further knowledge about curvature coordinates.

We can rewrite equation (3.14) in terms of these new coordinates keeping in mind that now $r = r(T, R)$ and $t = f(T, R)$.

$$\rho(T, R) = \frac{1}{4\pi R^2 R'} (M_{,T} T' + M_{,R} R') = \frac{1}{4\pi R^2} \left(M_{,R} + M_{,T} \frac{T'}{R'} \right). \quad (3.45)$$

To proceed we need to find an expression for the ratio T'/R' as a function of T and R only. To do so we consider the Jacobian of the transformation $(t, r) \rightarrow (T, R)$:

$$\frac{\partial(t, r)}{\partial(T, R)} = \begin{pmatrix} f_{,T} & f_{,R} \\ r_{,T} & r_{,R} \end{pmatrix} \quad (3.46)$$

$$\frac{\partial(T, R)}{\partial(t, r)} = \begin{pmatrix} \dot{T} & T' \\ \dot{R} & R' \end{pmatrix} \quad (3.47)$$

as they are one the inverse of the other, we get the set of equations:

$$\begin{cases} \dot{T} f_{,T} + T' r_{,T} = 1 \\ \dot{T} f_{,R} + T' r_{,R} = 0 \\ \dot{R} f_{,T} + R' r_{,T} = 0 \\ \dot{R} f_{,R} + R' r_{,R} = 1 \end{cases}. \quad (3.48)$$

Solving for T'/R' , taking into account (3.33) and (3.36), we find:

$$\frac{T'}{R'} = -\frac{f_{,R}}{f_{,T}} = \pm \frac{1}{A} \sqrt{\frac{1-A}{F}}. \quad (3.49)$$

As we are dealing with a gravitational collapse, we will take the negative root corresponding to $\dot{R} < 0 \Leftrightarrow \dot{R} = -\sqrt{1-A}$, and also $f_{,T} > 0$, which from equation (3.30) means that both times t and T , run in the same direction, at fixed R . Hence, equation (3.14) takes the form:

$$\rho(T, R) = \frac{1}{4\pi R^2} \left(M_{,R} - M_{,T} \frac{1}{A} \sqrt{\frac{1-A}{F}} \right). \quad (3.50)$$

The mass function must also satisfy another equation given by the fact that in the former coordinates it depends only on the radial coordinate, in fact:

$$\frac{\partial}{\partial t} M(r) = 0 \implies M_{,T} \dot{T} + M_{,R} \dot{R} = 0. \quad (3.51)$$

As usual we know \dot{R} as a function of T and R via (3.13) and to find $\dot{T}(T, R)$ we consider again the Jacobian of the transformation, solving (3.48) for \dot{T} we find after

some algebra:

$$\dot{T} = \frac{1 - \dot{R}f_R}{f_T} \implies \dot{T} = [A\sqrt{F}]^{-1} \quad (3.52)$$

where once again use has been made of the notation of (3.36) and equation (3.33). Therefore, we find the crucial constraint that the mass function has to satisfy in these coordinates.

$$M_{,T} - A\sqrt{(1-A)FM_{,R}} = 0. \quad (3.53)$$

Plugging this into (3.14) we finally arrive at:

$$4\pi\rho(T, R) = A(T, R)\frac{M_{,R}(T, R)}{R^2}. \quad (3.54)$$

We can now combine this equation with (3.42):

$$4\pi\rho R^2 = 4\pi A\rho R^2 u^T u_T \implies (u^T u_T)(T, R) = A(T, R)^{-1}, \quad (3.55)$$

from the normalization condition of timelike geodesics, we then find:

$$g_{\mu\nu}u^\mu u^\nu = 1 \implies u_R u^R = 1 - u_T u^T = 1 - A^{-1}. \quad (3.56)$$

Therefore, the expressions that determine the solution take the final form:

$$\begin{cases} M(T, R) = m + 4\pi \int_{R_0}^R d\tilde{R} \frac{\tilde{R}^2 \rho(T, \tilde{R})}{1 - 2M(T, \tilde{R})/\tilde{R} - \tilde{R}^2/l^2} \\ F(T, R) = \exp \left\{ 8\pi \int_{R_0}^R d\tilde{R} \tilde{R} \rho(T, \tilde{R}) \frac{1 + 2M(T, \tilde{R})/\tilde{R} + \tilde{R}^2/l^2}{(1 - 2M(T, \tilde{R})/\tilde{R} - \tilde{R}^2/l^2)^2} \right\} \end{cases}. \quad (3.57)$$

One of the advantages of these coordinates is that it is trivial to recover SdS in the vacuum limit: the integration functions have been chosen in such a way that setting $\rho(T, R) = 0$ in equations (3.57) leads to $M(T, R) = m$ and $F(T, R) = 1$. Therefore, the metric (3.36) reduces precisely to SdS (2.25).

We conclude this section with the corresponding remark made at the end of the previous section. In this scenario a particular solution is determined given a specific energy density profile $\rho(T, R)$ so that we are left with the following differential equations:

$$\begin{cases} M_{,R} = 4\pi \frac{R^3 \rho}{R(1 - R^2/l^2) - 2M} \\ M(T, R_0) = m \end{cases} \begin{cases} F_{,R} = 8\pi F R^2 \rho \frac{R(1 + R^2/l^2) + 2M}{[R(1 - R^2/l^2) - 2M]^2} \\ F(T, R_0) = 1 \end{cases} \quad (3.58)$$

where R_0 will be chosen according to the physical model we depicted at the beginning of the chapter, namely we will choose R_0 larger than the size of the galactic disk, so that we will have a description of the galaxy consistent with the form of $T_{\mu\nu}$. Finally, we want to emphasize that m , from the above equations, has the interpretation of the mass enclosed inside a shell of radius R_0 , so on physical terms we can assume it to be of the same order of the luminous mass of the galaxy.

3.3.1 Circular Geodesics

Let us now study the circular geodesics in this geometry, we will employ curvature coordinates, as they are more convenient and allow an easier visualization than the comoving ones.

We consider a test particle with coordinates $x^\mu = (T(s), R(s), \vartheta(s), \varphi(s))$ parametrized by the proper time s . As usual, the geodesics are given by:

$$\begin{cases} \frac{dv^\mu}{ds} + \Gamma_{\alpha\beta}^\mu v^\alpha v^\beta = 0 \\ v^\mu(s) = \frac{dx^\mu}{ds} \\ g_{\mu\nu} v^\mu v^\nu = 1 \end{cases} \quad (3.59)$$

and we can restrict our attention to orbits on the equatorial plane, setting $\vartheta(s) = \pi/2$. We are left with the non-vanishing Christoffel symbols:

$$\Gamma_{00}^0 = \frac{1}{2} \left(\frac{A_{,T}}{A} + \frac{F_{,T}}{F} \right) \quad \Gamma_{01}^0 \equiv \Gamma_{10}^0 = \frac{1}{2} \left(\frac{A_{,R}}{A} + \frac{F_{,R}}{F} \right) \quad \Gamma_{11}^0 = -\frac{\dot{A}}{2A^3F} \quad (3.60)$$

$$\Gamma_{00}^1 = \frac{A}{2} (AF)_{,R} \quad \Gamma_{01}^1 \equiv \Gamma_{10}^1 = -\frac{A_{,T}}{2A} \quad \Gamma_{11}^1 = -\frac{A_{,R}}{2A} \quad \Gamma_{33}^1 = -RA \quad (3.61)$$

$$\Gamma_{13}^3 \equiv \Gamma_{31}^3 = \frac{1}{R}. \quad (3.62)$$

Substituting in (2.47) we find the geodesic equations:

$$\begin{cases} \ddot{T} = -\frac{1}{2} \left(\frac{A_{,T}}{A} + \frac{F_{,T}}{F} \right) \dot{T}^2 - \left(\frac{A_{,R}}{A} + \frac{F_{,R}}{F} \right) \dot{T}\dot{R} + \frac{\dot{A}}{2A^3F} \dot{R}^2 \\ \ddot{R} = -\frac{A}{2} (AF)_{,R} \dot{T}^2 + \frac{A_{,T}}{A} \dot{T}\dot{R} + \frac{A_{,R}}{2A} \dot{R}^2 + AR\dot{\varphi}^2 \\ \ddot{\varphi} = -2\frac{\dot{R}}{R}\dot{\varphi} \\ v_\mu v^\mu = 1 \end{cases} \quad (3.63)$$

where the dot derivative stands now for the derivative with respect to the proper time of the particle.

Just like in SdS solution we can already perform an integration given the azimuthal symmetry of the solution: $\dot{\varphi} = -J/R^2$, where J is the integral of motion, i.e. the angular momentum per unit mass.

Considering this, we arrive at the independent set of geodesic equations:

$$\begin{cases} \ddot{T} = -\frac{1}{2} \left(\frac{A_{,T}}{A} + \frac{F_{,T}}{F} \right) \dot{T}^2 - \left(\frac{A_{,R}}{A} + \frac{F_{,R}}{F} \right) \dot{T}\dot{R} + \frac{\dot{A}}{2A^3F} \dot{R}^2 \\ \ddot{R} = -\frac{A}{2} (AF)_{,R} \dot{T}^2 + \frac{A_{,T}}{A} \dot{T}\dot{R} + \frac{A_{,R}}{2A} \dot{R}^2 + \frac{A}{R^3} J^2 \\ \dot{\varphi} = 2\frac{\dot{R}}{R^3} J^2 \\ v_\mu v^\mu = 1 \end{cases} \quad (3.64)$$

To obtain circular geodesics we fix a certain value for the radial motion $R(s) = R$ hence the geodesics must satisfy:

$$\begin{cases} \dot{T} = -\frac{1}{2} \left(\frac{A_{,T}}{A} + \frac{F_{,T}}{F} \right) \dot{T}^2 \\ 0 = -\frac{A}{2} (AF)_{,R} \dot{T}^2 + \frac{A}{R^3} J^2 \\ \dot{\phi} = 0 \\ v_\mu v^\mu = 1 \Leftrightarrow AF \dot{T}^2 - \frac{J^2}{R^2} = 1 \end{cases} . \quad (3.65)$$

Combining the information of the second and fourth equation we can solve for \dot{T} and eliminating it we find the expression for the rotation curve:

$$\frac{J^2}{R^2} \equiv v_\phi^2 = \left[\frac{2}{R} \frac{AF}{(AF)_{,R}} - 1 \right]^{-1} . \quad (3.66)$$

Recovering the definitions (3.36) and taking into account the differential relation (3.54) it becomes:

$$v_\phi^2(R) = \left[\frac{\left(1 - \frac{2M(T,R)}{R} - \frac{R^2}{l^2} \right)^2}{4\pi R^2 \rho(T,R) - \left(1 - \frac{2M(T,R)}{R} - \frac{R^2}{l^2} \right) \left(4\pi R^2 \rho(T,R) - \frac{M(T,R)}{R} + \frac{R^2}{l^2} \right)} - 1 \right]^{-1} . \quad (3.67)$$

Before analyzing this expression, let us make some remarks. First, we note that this quantity is the same in the comoving coordinates as the transformation introduced in the previous section maps φ into ϕ , and the proper time s is invariant. We can also see how the SdS behavior (2.60) is recovered in the vacuum limit, in fact setting $\rho(T,R) = 0$ we get:

$$v_\phi^2(R) = \left[\frac{1 - \frac{2m}{R} - \frac{R^2}{l^2}}{\frac{m}{R} - \frac{R^2}{l^2}} - 1 \right]^{-1} = \frac{m - R^3/l^2}{R - 3m} . \quad (3.68)$$

However the expression (3.67) has a huge problem: the left hand side must be a function of R only, as J is an integral of motion, but the right hand side has functional dependence on T , given by the mass and energy density function. In principle, there is no reason why the right hand side would depend solely on R , except, for the SdS case, and therefore (3.67) is inconsistent.

What this tells us is that circular geodesics do not exist for spherically inhomogeneous LT models. This conclusion is not actually so surprising in fact we recall that the mass function $M(T,R)$, for fixed R , is nothing but the active gravitational mass enclosed on a shell of that areal radius, and it evolves in time accordingly with the fluid dynamics. This time dependence has to be present as the constraint equation (3.53) must be satisfied.

For example let us consider ad absurdum the case $M_{,T} = 0 \implies M = M(R)$ this

would lead to:

$$M_{,R} = 0 \implies M = m \Leftrightarrow SdS \quad (3.69)$$

∨

$$A = 1 \implies \frac{2M(R)}{R} + \frac{R^2}{l^2} = 0. \quad (3.70)$$

The first case has a solution and it has already been discussed, the second case instead has no solution but let us see in more detail what it means. From equation (3.55) we can write:

$$u_T = g_{TT}u^T \implies AF(u^T)^2 = 1/A \quad (3.71)$$

So from the timelike normalization we find:

$$AF(u^T)^2 - \frac{(u^R)^2}{A} = 1 \implies (u^R)^2 = 1 - A, \quad (3.72)$$

therefore the condition $A = 1$ implies a static cloud of dark matter, which is intuitively what would be needed to have circular geodesics.

To summarize, we are left with only two options: either the mass function is a constant, and there can be circular geodesics, or it depends on both position and time, so that the halo must evolve and truly circular geodesics cannot exist.

However not everything is lost, we always have to remind ourselves that we are describing a physical system of which we know the physics thanks to observations, for instance we know that there exist physical orbits that are circular with very good approximation. In our framework this means that the radial geodesic velocity of the fluid $u^R(T, R)$, which must depend on time, has to be negligible for all times and positions we consider. In fact, this statement is in good agreement with the steady-state assumption for galaxies that we have discussed in the first chapter.

Let us see in little more detail the specific situation we are dealing with.

$$u^R(T, R) \ll 1 \Leftrightarrow \frac{2M(T, R)}{R} + \frac{R^2}{l^2} \ll 1. \quad (3.73)$$

For this to hold we see that the following condition must be satisfied for all times:

$$M(T, R) \ll R \ll l. \quad (3.74)$$

The timescale on which the mass function varies is given by:

$$\tau = \frac{M}{M_{,T}} = \frac{M}{AM_{,R}\sqrt{F(1-A)}}. \quad (3.75)$$

Plugging in the condition (3.54) it becomes:

$$\tau = \frac{M}{M_{,T}} = \frac{M}{4\pi R^2 \rho \sqrt{F(1-A)}}. \quad (3.76)$$

To estimate this quantity, with (3.74) in mind, we consider $M_{,R} \approx M/R$ which is consistent with the Newtonian behavior of flat rotation curves $M \propto R$. From (3.54)

and (3.57) we then get:

$$\begin{cases} R^2\rho \approx \frac{M}{4\pi R} \\ \frac{F_{,R}}{F} = 8\pi R\rho \frac{2-A}{A^2} \approx 8\pi R\rho \approx \frac{2M}{R^2} \end{cases} \quad (3.77)$$

From the second equation we can approximate $F \approx 1$ since it is smaller than M/R . We get the timescale of the order:

$$\tau \approx \frac{R}{\sqrt{\frac{2M}{R} + \frac{R^2}{l^2}}} \quad (3.78)$$

This quantity has to be compared with the observational time which is of order $\tau_{obs} \approx 1yr$, i.e., in our units $\tau_{obs} \approx 0.3pc$. The steady-state condition $\tau \gg \tau_{obs}$ is met if:

$$\frac{R}{\sqrt{\frac{2M}{R} + \frac{R^2}{l^2}}} \gg 0.3 \times 10^{-3}kpc \implies R \gg 10^{-2}M^{1/3}kpc^{2/3} \quad (3.79)$$

In the worst case, where M reaches the order of a galaxy cluster (at most $10^{15}M_{\odot}$ i.e. $0.5 \times 10^{-1}kpc$) we would need $R \gg 0.5^{1/3} \times 10^{-2}10^{-1/3}kpc \approx 10^{-3}kpc$ which is always satisfied as it is extremely unlikely to find such high mass values within radii of $1pc$. Hence in the regime given by (3.74) the time scale on which the mass function varies, for fixed R , is much larger than the time scale for which we have access to the system, therefore we can introduce the reasonable simplifying working hypothesis of neglecting all time dependences, and study circular geodesics from equation (3.67). To conclude this section let us rewrite equation (3.67) in such regime. To do so we will consider only terms of order M/R and R^2/l^2 , neglecting cross products and higher powers in the expansion. We begin considering the quantity with functional dependence in the denominator.

$$\begin{aligned} v_{\phi}^{-2} + 1 &= \frac{(1 - 2M/R - R^2/l^2)^2}{4\pi R^2\rho - (1 - 2M/R - R^2/l^2)(4\pi R^2\rho - M/R + R^2/l^2)} \approx \\ &\approx \frac{1 - 4M/R - 2R^2/l^2}{M/R(1 + 8\pi R^2\rho) - R^2/l^2(1 - 4\pi R^2\rho)} \end{aligned} \quad (3.80)$$

Again considering that $R^2\rho$ is of order M/R we can neglect the terms in the brackets compared to one as they would lead to higher orders corrections. We find therefore the velocity:

$$\begin{aligned} v_{\phi}^2 &= \left[\frac{(1 - 2M/R - R^2/l^2)^2}{4\pi R^2\rho - (1 - 2M/R - R^2/l^2)(4\pi R^2\rho - M/R + R^2/l^2)} - 1 \right]^{-1} \approx \\ &\approx \left[\frac{1 - 4M/R - 2R^2/l^2}{M/R(1 + 8\pi R^2\rho) - R^2/l^2(1 - 4\pi R^2\rho)} - 1 \right]^{-1} \\ &\approx \frac{M/R - R^2/l^2}{1 - 5M/R - R^2/l^2} \end{aligned} \quad (3.81)$$

. Finally

$$v_\varphi = \sqrt{\frac{M}{R} - \frac{R^2}{l^2}} \left(1 + \frac{5}{2} \frac{M}{R} + \frac{1}{2} \frac{R^2}{l^2} \right). \quad (3.82)$$

Let us now make some consideration about this formula.

We first notice the same behavior found for SdS circular geodesics: for increasingly higher values of R the rotation velocity decreases as the dark energy contribution gets more dominant, until eventually this will be so large that the velocity goes to zero and will not be defined for larger values of R . For an immediate visualization of the values at which this phenomenon happens let us define $\tilde{M}(R)$ the corresponding mass that must be reached as a function of the distance:

$$v_\varphi = 0 \Leftrightarrow \frac{\tilde{M}}{R} - \frac{R^2}{l^2} = 0 \implies \tilde{M}(R) = \frac{R^3}{l^2}. \quad (3.83)$$

If for a given R , the mass reached as a solution of (3.54), is higher than this value, then the velocity is still defined. Let us consider for example the distance of one megaparsec, as it is a typical distance between galaxies. In order to have the cosmological constant contribution so relevant that the circular geodesics break down at this radius we need to match a mass of:

$$\tilde{M}(1Mpc) = \frac{(1Mpc)^3}{l^2} \approx 3 \times 10^{-5} kpc \approx 6 \times 10^{11} M_\odot. \quad (3.84)$$

Let us now study the derivative of (3.82). In the regime of (3.74) the leading order is given by:

$$v'_\varphi(R) = \frac{1}{2v_\varphi} \left(\frac{M'}{R} - \frac{M}{R^2} - \frac{2R}{l^2} \right). \quad (3.85)$$

Taking into account (3.54) we find the critical value:

$$4\pi R^2 \rho = \frac{M_*}{R} + 2 \frac{R^2}{l^2} \Leftrightarrow M_* = 2R^3(2\pi\rho - l^{-2}) \quad (3.86)$$

where again we found convenient to define the mass value at which this condition is met. Until the mass function is smaller than M_* , the velocity is increasing; a plateau will be reached when the mass function meets M_* , and the velocity will be decreasing if it assumes higher values.

3.4 Numerical Analysis

To fully compute the rotation curves in the LT geometry via (3.82) we need to determine the mass function. We can rewrite equations (3.58) in our approximation as:

$$\begin{cases} M_{,R} = 4\pi \frac{R^3 \rho}{R(1 - R^2/l^2) - 2M} \\ M(R_0) = m \end{cases} \quad (3.87)$$

Given the nonlinearity of the equation we have to resort to numerical integration to find a solution, moreover, we remark that the equation for F is irrelevant at this point

since we have already shown it is of a higher order than M/R .

As we have anticipated, the solution to (3.87) is fully specified given an energy density profile, therefore, to proceed in the discussion we need to pick a realistic profile for $\rho(R)$, that properly describes the observed characteristics of the dark halo.

Since the only clue we have about dark matter is that it interacts gravitationally, we know from the Newtonian arguments presented in the first chapter that flat rotation curves are obtained if the mass of the halo increases linearly with the radius at large distances from the luminous part. This in turn means that the halo density has asymptotic behavior R^{-2} . The natural ansatz to reproduce flat rotation curve is therefore given by:

$$\rho^{FR}(R) = \frac{\rho_0^{FR}}{1 + (R/\alpha_{FR})^2}, \quad (3.88)$$

where we have assumed a core density ρ_0 and a parameter α related to the size of the halo. In the following we will refer to this density profile as FR profile, as it leads to flat rotation curves.

A more accurate profile is given by the Navarro-Frenk-White profile (see J.F. Navarro, 1996), obtained with N-body simulation:

$$\rho^{NFW}(R) = \frac{\rho_0^{NFW}}{(R/\alpha_{NFW})(1 + R/\alpha_{NFW})^2}. \quad (3.89)$$

Both these formulas are valid only for the values of R for which the LT geometry is valid, i.e. referring to (3.87), for $R \geq R_0$.

Moreover we are not completely free to choose the parameters, in fact, as we want to match the observations of flat rotation curves, we must request that $v_\varphi(R)$ starts as a monotonically increasing function of R , and is almost flat for $R = R_0$. Keeping in mind the discussion at the end of the previous section we see that thanks to (3.86) this translates to:

$$M(R_0) = m \approx M_*(R_0) \Leftrightarrow \rho(R_0) \approx \frac{m + 2R_0^3/l^2}{4\pi R_0^3} \approx \frac{m}{4\pi R_0^3} \quad (3.90)$$

as the cosmological constant is insignificant at this scale.

This constraint allows us to adjust the core density value, as we already know the order of magnitude of the central mass m :

$$\begin{cases} \rho_0^{FR} \approx \frac{m}{4\pi R_0^3} (1 + (R_0/\alpha_{FR})^2) \\ \rho_0^{NFW} \approx \frac{m}{4\pi R_0^2 \alpha_{NFW}} (1 + R_0/\alpha_{NFW})^2 \end{cases}. \quad (3.91)$$

However we cannot set arbitrarily high values as we have in any case to match the observed value of $v_\varphi \approx 200 \text{ km/s}$.

Referring to the Table 1.1 we assume the following parameters for the halo scale and the enclosed central mass:

$$\begin{cases} m = 6 \times 10^{-6} \text{ kpc} \\ R_0 = 20 \text{ kpc} \end{cases}. \quad (3.92)$$

In turn the density profile parameters we have chosen are:

$$\begin{cases} \alpha_{FR} = 2.4 \text{ kpc} \\ \rho_0^{FR} = 9.2 \times 10^{-9} \text{ kpc}^{-2} \\ \alpha_{NFW} = 19.3 \text{ kpc} \\ \rho_0^{NFW} = 1.6 \times 10^{-10} \text{ kpc}^{-2} \end{cases} . \quad (3.93)$$

The values of such parameters do not have any particular physical meaning, they have been chosen merely to reproduce as good as possible the observation data presented in Table 1.1 and in Figure 1.3.

We display here the plots of the rotation curves for both profiles until a distance of $R = 40 \text{ kpc}$ from the galactic center, which is typically the order of the last measured point (see Table 1.1).

FIGURE 3.1: Rotation curve for FR profile.

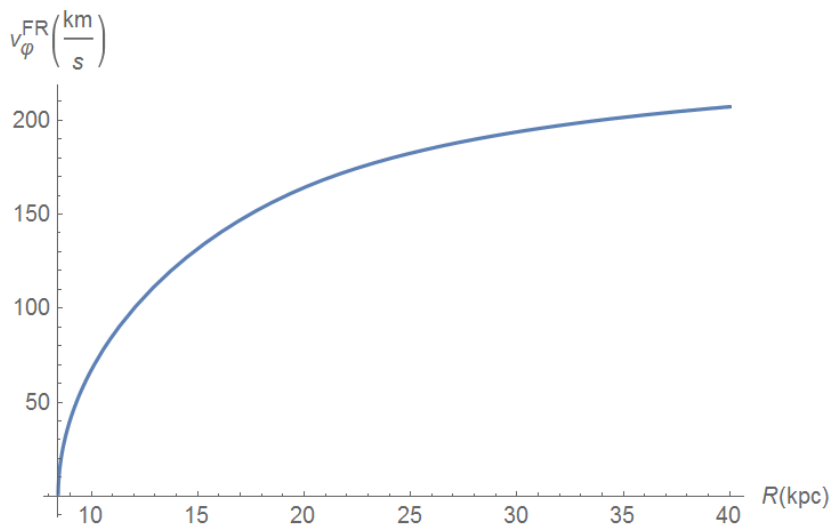
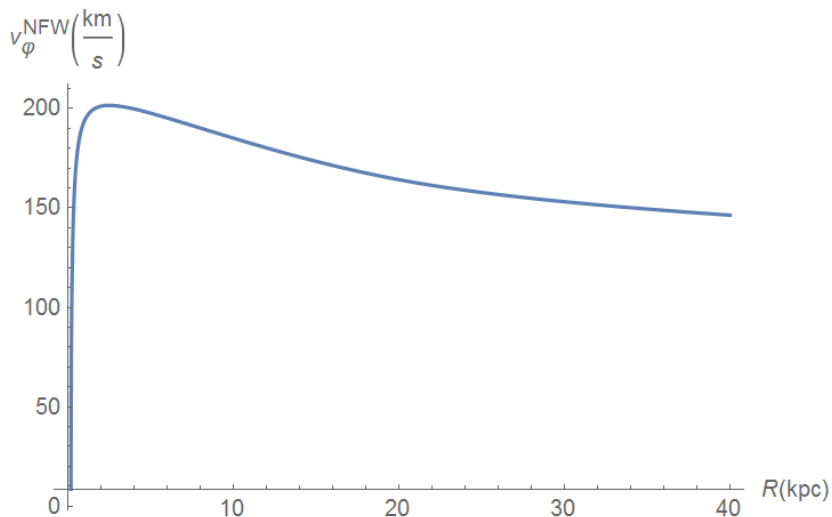


FIGURE 3.2: Rotation curve for NFW profile.



To get a comparison with the figures we have suppress the calculations and extrapolated the values to obtain rotation curves for $R < R_0$. In both cases, we see an agreement with the figures in 1.3.

Let us now focus our attention to the more interesting part of the plot, i.e. $R \gg R_0$ where we can actually see the cosmological constant's effect.

We show here the plots in the case of vanishing and non-vanishing cosmological constant.

FIGURE 3.3: Rotation curve for FR profile for vanishing and non-vanishing Λ at large radii.

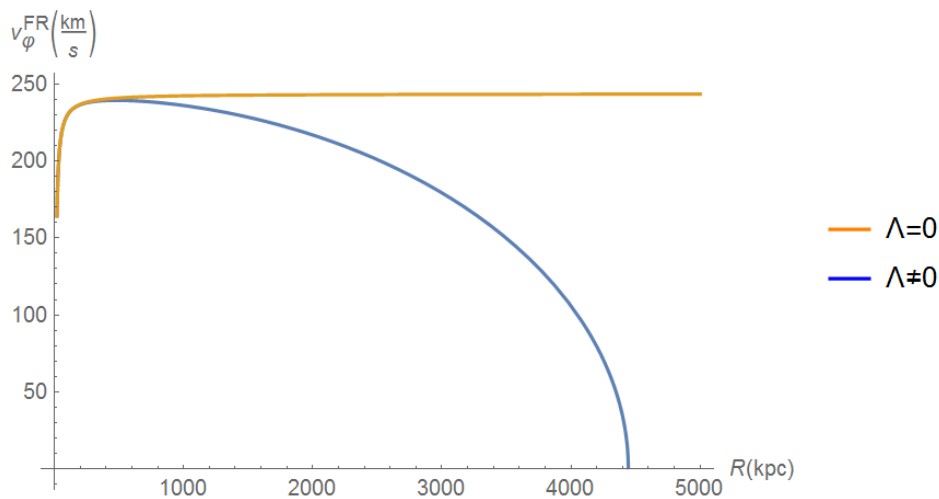
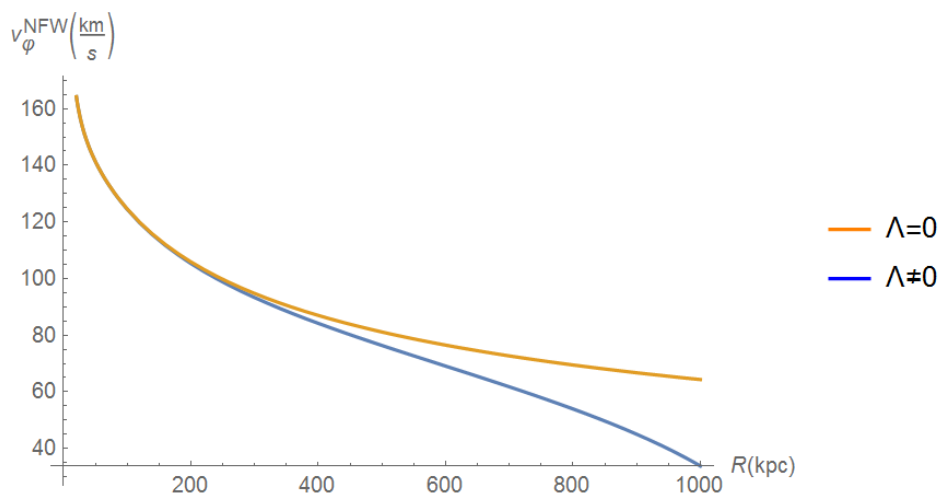
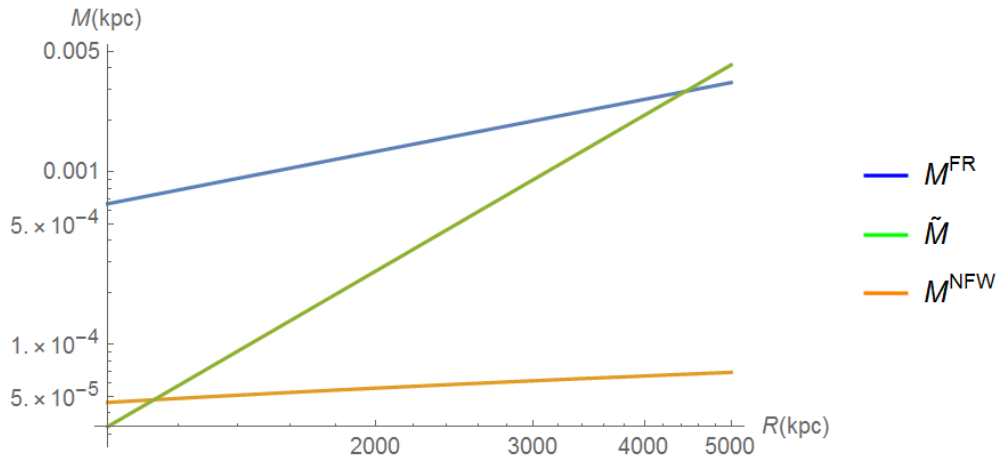


FIGURE 3.4: Rotation curve for NFW profile for vanishing and non-vanishing Λ at large radii.



To see for which values the circular geodesics break we have to determine for which radius M matches \tilde{M} . This situation is illustrated with the following graph.

FIGURE 3.5: Behaviors of the mass functions with both profiles and \tilde{M} in bilogarithmic scale.



Numerically we find the values:

$$\begin{cases} M^{FR} = \tilde{M}^{FR} \Leftrightarrow R_{max}^{FR} = 4.4 Mpc \\ M^{NFW} = \tilde{M}^{NFW} \Leftrightarrow R_{max}^{NFW} = 1.1 Mpc \end{cases} . \quad (3.94)$$

As expected $R_{max}^{FR} > R_{max}^{NFW}$ since the mass function grows more rapidly in the case of FR profile than the NFW one.

We do the same for M and M_* and we find:

$$M^{FR} = M_*^{FR} \Leftrightarrow R_{crit}^{FR} = 480 kpc . \quad (3.95)$$

As the NFW profile does not produce flat rotation curves we do not display R_{crit}^{FR} since it is not related to the presence of the cosmological constant. However we can give a rough estimate of the scale at which Λ becomes relevant looking at the Figure 3.4, from which we see it is of order $200 kpc$. For the FR profile, instead, R_{crit} gives a good estimate because in the case $\Lambda = 0$ the velocity never decreases.

Conclusions

This work has aimed to address the study of galactic rotation curves in the Λ CDM framework of cosmology, investigating, in particular, the role of the cosmological constant on rotation curves.

At first, we recalled the main principles on which the standard model of cosmology is based upon, and then we coherently applied these to the description of an isolated galaxy in the Universe. We started with a simplified model in which the galaxy's components experience their dynamics in the vacuum; this automatically leads to the SdS spacetime, where the galaxy has the role of the black hole. Circular geodesics have been studied and we found analytical results in the same fashion of Schwarzschild spacetime. The substantial difference, given by the cosmological constant, is that the angular momentum of orbiting test particles is defined until a maximum radius $R_{max} = (ml^2)^{1/3}$. For a galaxy of total mass $10^{11}M_{\odot}$, this is of the order of half megaparsec. Moreover, the rotation curve given by the function (2.60) is not flat, and we can see that the cosmological constant's contribution starts to kick in when this function changes concavity, at roughly $R_{flex} = 0.3Mpc$.

This result motivates the need for a more realistic description that takes into account the environment in which geodesics occur, in particular the dark halo, as we expect Λ to have effects at such large scales. To do so, we considered the galactic geometry to be LT on scales where the luminous part could be neglected, but still taking it into account as a central mass. Studying circular geodesics we arrived at an expression for v_{φ} that can approximate the real condition of steady-state galaxies, in particular for it to be a good approximation we need (3.74) to hold. Working in this regime we assumed the validity of (3.82) to describe the rotation curve.

We investigated this formula for two density profiles: one is the naive ansatz to reproduce the flat rotation curves; the other is the well known NFW profile, which is the most successful tool from numerical simulations of dark halos. In both cases, the effect of the cosmological constant is to progressively reduce the circular velocity, until these geodesics are no longer defined. The extent of this effect can again be seen studying the critical values of v_{φ} in comparison with the case of vanishing Λ : for the naive ansatz, we find that the cosmological constant kicks in for roughly $0.4Mpc$ while for the NFW profile for $0.2kpc$. The maximal radii we have found are approximately $4Mpc$ in the former case, and $1Mpc$ in the latter.

We can, therefore, conclude that in the theory presented here the cosmological constant indeed plays a fundamental role for galactic rotation curves. However to see the effect experimentally we need an isolated galaxy, in which the spherical symmetry is as respected as possible. The requirement of having an isolated galaxy lies in the fact that the extent of the cosmological constant's effect is already of the order of where usually another galaxy begins.

To conclude on a positive note we would like to point out that an actual observation of this effect would allow us to obtain an independent measurement of the cosmological

constant, which could potentially shed new light on the dark energy problem.

Appendix A

Nariai solution

Let us consider a flat six-dimensional Minkowski space with line element:

$$ds^2 = (dX_0)^2 - \sum_{i=1}^5 (dX_i)^2 \quad (\text{A.1})$$

The Nariai space can be conveniently constructed considering two constraints in this space:

$$\begin{cases} -(X_0)^2 + (X_1)^2 + (X_2)^2 = R^2 \\ (X_3)^2 + (X_4)^2 + (X_5)^2 = R^2 \\ R^2 = 1/\Lambda \end{cases} \quad (\text{A.2})$$

We immediately recognize from the first constraint the equation of a hyperboloid in three dimensions, and from the second the equation of a sphere living in a three dimensional space.

Since we know that the de Sitter metric is the induced metric from the standard flat metric on a hyperboloid, we can conclude that the Nariai spacetime is the direct product $dS_2 \times S^2$ and, as a consequence, it admits a six-dimensional group of isometries $SO(2,1) \times SO(3)$.

Let us now see some four-dimensional parametrization of the Nariai solution.

For $0 < r < R$ the following parametrization

$$\begin{cases} X_0 = \sqrt{R^2 - r^2} \sinh(t/R) \\ X_1 = \sqrt{R^2 - r^2} \cosh(t/R) \\ X_2 = r \\ X_3 = R \sin \theta \cos \varphi \\ X_4 = R \sin \theta \sin \varphi \\ X_5 = R \cos \theta \end{cases} \quad (\text{A.3})$$

leads to

$$ds^2 = \left(1 - \frac{r^2}{R^2}\right) dt^2 - \left(1 - \frac{r^2}{R^2}\right)^{-1} dr^2 - R^2(d\theta^2 + \sin^2 \theta d\varphi^2) \quad (\text{A.4})$$

With a natural re-definition, for $\tau \in (-\infty, +\infty)$ and $\chi \in [0, 2\pi]$ via

$$\begin{cases} X_0 = R \sinh(\tau/R) \\ X_1 = R \cosh(\tau/R) \cos \chi \\ X_2 = R \cosh(\tau/R) \sin \chi \end{cases} \quad (\text{A.5})$$

we obtain the already shown

$$ds^2 = d\tau^2 - \cosh^2(\tau/R)d\chi^2 - R^2(d\theta^2 + \sin^2\theta d\varphi^2) \quad (\text{A.6})$$

A peculiar property of this solution is that it can be obtained as a limit of SdS spacetime. As we already discussed the SdS spacetime presents both a black hole horizon and a cosmological horizon, the position of these two is actually a function of the mass m and there exist a value for which the two horizons coincide. It turns out that with a proper limiting procedure this would lead precisely to the Nariai solution (references for this appendix can be found in K.G. Begeman, 1991 and Ortaggio, 2001).

Bibliography

- Durrer, R. (2008). *The Cosmic Microwave Background*. Cambridge University Press.
- Hawley J. F., Holcomb K. A. (2005). *Foundations of Modern Cosmology*. OUP Oxford.
- J. Binney, M. Marrifield (1998). *Galactic Astronomy*. Princeton Series in Astrophysics. Princeton University Press.
- J. Binney, S. Tremaine (1987). *Galactic Dynamics*. Princeton Series in Astrophysics. Princeton University Press.
- J. Plebanski, A. Krasinski (2006). *An Introduction to General Relativity and Cosmology*. Cambridge University Press.
- J.F. Navarro C.S. Frenk, S.D.M. White (1996). "The Structure of Cold Dark Matter Halos". In: *The Astrophysical Journal*. 462: 563. URL: [arXiv:astro-ph/9508025](https://arxiv.org/abs/astro-ph/9508025).
- K.G. Begeman A.H. Broeils, R.H. Sanders (1991). "Extended rotation curves of spiral galaxies - Dark haloes and modified dynamics". In: *Monthly Notices of the Royal Astronomical Society (ISSN 0035-8711)*, vol. 249, April 1, 1991, p. 523-537.
- L. Amendola, S. Tsujikawa (2010). *Dark Energy: Theory and Observations*. Cambridge University Press.
- Maeder, Andre; et al. (DES Collaboration) (2018a). "First Cosmology Results using Type Ia Supernovae from the Dark Energy Survey: Constraints on Cosmological Parameters". In: *The Astrophysical Journal*. 872 (2): L30.
- Maeder, Andre; et al. (Planck Collaboration) (2018b). "Planck 2018 results. VI. Cosmological parameters". In: URL: [arXiv:1807.06209](https://arxiv.org/abs/1807.06209) [[astro-ph](https://arxiv.org/abs/astro-ph).CO].
- Newton, I. (1713). *Philosophiae Naturalis Principia Mathematica*.
- Ortaggio, M. (2001). "Impulsive waves in the Nariai universe". In: *Phys.Rev. D*65 (2002) 084046. URL: [arXiv:gr-qc/0110126](https://arxiv.org/abs/gr-qc/0110126).
- Peeble, P.J.E (1993). *Principles of Physical Cosmology*. Princeton Series in Physics. Princeton University Press.
- Planck (2018). "Planck 2018 results. VI. Cosmological parameters". In: URL: [arXiv:1807.06209](https://arxiv.org/abs/1807.06209).
- Planck, M. (1968). *Scientific Autobiography and Other Papers*.
- Ptolemaeus, C. (c. 150 AD). *Almagestum*.
- Straumann, N. (2005). *General Relativity*. Graduate Texts in Physics. Springer Verlag.
- V.C. Rubin W.K. Ford, N. Thonnard (1980). "Rotational properties of 21 SC galaxies with a large range of luminosities and radii, from NGC 4605 /R = 4kpc/ to UGC 2885 /R = 122 kpc/". In: *The Astrophysical Journal, Part 1*, vol. 238, June 1, 1980, p. 471-487.